

**THE ROLE OF ERBB INHIBITORS IN PROMOTING NERVE
REGENERATION IN A MOUSE MODEL OF NERVE INJURY**

by

Jacob Stewart Peller

A thesis submitted to the Graduate Program in Neuroscience
in conformity with the requirements for the
Degree of Master of Science

Queen's University
Kingston, Ontario, Canada

July 2021

© Jacob Peller, 2021

Abstract

Nerve injury is a common clinical challenge that has a considerable impact on an individual's quality of life and function. Despite multiple surgical strategies, functional outcomes following nerve injury remain poor. Increasing the rate at which axons regenerate could profoundly improve the success of recovery. The goal of this thesis was to investigate whether the dual ErbB1-ErbB2 inhibitor lapatinib or the ErbB1 inhibitor gefitinib could promote nerve regeneration in both *in vivo* and *in vitro* models. Using a mouse transection and repair sciatic nerve injury model, lapatinib was found to increase the number of regenerated myelinated axons at 28 days following nerve repair. For elucidation of the molecular pathway that could be promoting nerve regeneration, *in vivo* neurite growth assays interestingly demonstrated that gefitinib, more than lapatinib rescued the inhibitory effects by chondroitin sulfate proteoglycan on neurite growth. Furthermore, a mouse forelimb model of nerve injury was characterized which can be used to study the cellular and molecular effects of ErbB inhibitors in transgenic mice. The repurposing of ErbB inhibitors to enhance nerve regeneration requires further study to determine whether this therapy could be translated to improve functional recovery in people with nerve injury.

Acknowledgements

I would like to thank my family, friends and partner for their support over the past two years during my MSc. I would also like to thank Dr. Michael Kawaja who mentored me during my undergraduate degree and captivated my interest in the nervous system. I am also incredibly grateful for Dr. Michael Hendry for recruiting me as his first graduate student after only just being introduced and am grateful for his guidance as I pursue a career as a physician-scientist. I would especially like to acknowledge the support over the past four years in the Kawaja lab by lab technicians Verna Norkum and Anne-Marie Crotty. Thank you as well to other graduate students – Honz, Hanin, Stevie and Bernie for their friendship in the lab over the past few years. Finally, I would like to thank the Canadian Institutes of Health Research (CIHR) which awarded me a Frederick Banting and Charles Best Canada Graduate Scholarship – Master’s (CGS-M) which funded this research.

Table of Contents

Abstract.....	ii
Acknowledgements.....	iii
Table of Contents.....	iv
List of Tables.....	vi
List of Figures.....	vii
List of Abbreviations.....	viii
Chapter 1: Introduction.....	1
Chapter 2: Literature Review.....	4
2.1 Nerve anatomy.....	4
2.1.1 Axons and Schwann cells.....	4
2.1.2 Connective tissue layers.....	8
2.2 Nerve injury.....	10
2.2.1 Classification of nerve injury.....	10
2.3 Nerve regeneration.....	12
2.3.1 Response of the neuron.....	13
2.3.2 Role of Schwann cells.....	14
2.3.3 Role of neurotrophic factors.....	15
2.3.4 Role of time and distance.....	16
2.3.5 Inhibitors of nerve regeneration.....	16
2.4 Treatment of nerve injury.....	17
2.4.1 Nerve transfer.....	18
2.5 ErbB family.....	20
2.5.1 ErbB1.....	21
2.5.2 ErbB2.....	21
2.5.3 ErbB3.....	22
2.5.4 ErbB4.....	22
2.6 ErbB inhibitors.....	21
2.6.1 Trastuzumab.....	23
2.6.2 Lapatinib.....	24
2.6.3 Gefitinib.....	24
2.7 Role of ErbB family in nerve regeneration.....	24

Chapter 3: Inhibition of the ErbB1 and ErbB2 receptors increases the number of regenerating myelinated axons in a mouse model of nerve injury.....	28
3.1 Introduction.....	28
3.2 Methods.....	29
3.2.1 Experimental design and animal numbers.....	29
3.2.2 Lapatinib and vehicle administration.....	30
3.2.3 Surgical procedures.....	30
3.2.4 Retrograde labelled tissue: harvesting, processing and analysis.....	31
3.2.5 Nerve histomorphometry.....	33
3.2.6 Neurite growth assay.....	33
3.2.7 Statistical analysis.....	34
3.3 Results.....	34
3.3.1 Animal survival.....	34
3.3.2 Lapatinib does not increase the number of regenerating sensory or motor neurons, 10- or 28-days following nerve repair.....	35
3.3.3 Lapatinib increases the number of regenerating myelinated axons following nerve repair.....	35
3.3.4 Gefitinib promotes neurite extension in cultured DRG neurons.....	36
3.4 Discussion.....	40
3.5 Conclusion.....	42
Chapter 4: Characterization of a mouse forelimb model of median nerve injury.....	44
4.1 Introduction.....	44
4.2 Methods.....	45
4.2.1 Experimental design and animal numbers.....	45
4.2.2 Retrograde labelling.....	46
4.2.3 Retrograde labelled tissue: harvesting, processing and analysis.....	46
4.2.4 Nerve histomorphometry.....	47
4.2.5 Forelimb grip strength.....	47
4.3 Results.....	48
4.3.1 Mouse median nerve gross anatomy.....	48
4.3.2 Quantification of the uninjured median nerve motor neuron pool.....	48
4.3.3 Median nerve histomorphometry.....	49
4.3.4 Forelimb grip strength.....	49
4.4 Discussion.....	52
4.5 Conclusion.....	54
Chapter 5: General discussions, conclusions and future directions.....	55
References.....	58

List of Tables

Table 2.1: Classification of nerve injury.....	12
Table 2.2: Overview of the ErbB family.....	21
Table 3.1: Summary of experiment groups and animal numbers in lapatinib nerve regeneration experiment.....	30

List of Figures

Figure 2.1 Molecular domains of a myelinated axon.....	6
Figure 2.2 Nerve histology.....	9
Figure 2.3 Nerve transfer coaptations.....	19
Figure 3.1 Surgical techniques.....	32
Figure 3.2 The number of regenerated sensory or motor neurons following sciatic nerve transection is not statistically different between lapatinib and vehicle treated mice.....	37
Figure 3.3 Administration of lapatinib increases the number of regenerated myelinated axons 28 days following nerve repair.....	38
Figure 3.4 Gefitinib rescues the effect of CSPG mediated neurite growth inhibition.....	39
Figure 4.1 The mouse brachial plexus.....	50
Figure 4.2 Retrograde labelled motor neurons of the median nerve.....	51
Figure 4.3 Median nerve histomorphometry.....	52
Figure 4.4 Forelimb grip strength following median nerve transection.....	53

List of Abbreviations

BBB: blood-brain barrier
BDNF: brain-derived neurotrophic factor
cAMP: cyclic-adenosine monophosphate
CNS: central nervous system
CNTF: ciliary neurotrophic factor
CREB: cAMP response element-binding protein
CSPG: chondroitin sulfate proteoglycan
DRG: dorsal root ganglion
EGF: epidermal growth factor
EGFR: epidermal growth factor receptor
FDA: Food and Drug Administration
GFAP: glial fibrillary acidic protein
GDNF: glial cell line derived neurotrophic factor
HB-EGF: heparin-binding epidermal growth factor
HER: human epidermal growth factor receptor
MAG: myelin-associated glycoprotein
NrCAM: neuronal cell adhesion molecule
NGF: nerve growth factor
NT-3: neurotrophin-3
NT-4: neurotrophin-4
NRG: neuregulin
PFA: paraformaldehyde
PKA: protein kinase A
PNS: peripheral nervous systems
TGF- α : transforming growth factor alpha

Chapter 1: Introduction

Functional recovery following nerve injury remains poor despite the advent of several surgical techniques for the repair of injured peripheral nerves. While axon regeneration in the central nervous system is limited, axons in the peripheral nervous system have a greater capacity to regenerate and restore functional connections. Increasing the rate of axonal regeneration and thus decreasing the time of chronic denervation of Schwann cells and chronic axotomy could profoundly improve time to recovery and success of functional reinnervation.¹ Numerous therapeutic strategies have been explored to increase the rate of nerve regeneration including neurotrophic factors, immunosuppressants and electrical stimulation. Despite this, there are no FDA-approved therapies that increase the rate of nerve regeneration. As reviewed in Chapter 2, the ErbB family has an important role in nerve regeneration² and recent experiments have demonstrated the potential for the ErbB2 inhibitor trastuzumab to promote regeneration in a rat model of peripheral nerve injury.³ The repurposing of an approved FDA therapy to nerve injury treatment could have an impact on the approximately 20 million people in the United States each year with nerve injuries and the associated \$20 billion cost to the healthcare system.^{4,5} Currently, no studies have conclusively elucidated the mechanism by which ErbB inhibitors may promote nerve regeneration, or investigated the use of small molecule ErbB inhibitors in *in vivo* models of nerve injury. The rationale for this thesis is thus based on two previous findings. First, that the ErbB family has a role in nerve regeneration and second, that ErbB inhibitors can promote regeneration following injury.^{3,6} We sought to expand on this work by further exploring the ability of two novel ErbB inhibitors to promote nerve regeneration following injury.

The primary goal of this thesis was to investigate the regulatory impact of the small molecule ErbB1-ErbB2 inhibitor lapatinib and ErbB1 inhibitor gefitinib on nerve regeneration

following injury (Chapter 3). Our main hypothesis was that both lapatinib and gefitinib would promote nerve regeneration by preventing a recently identified inhibitory dimerization between the ErbB1-ErbB2 heterodimer.³ A secondary goal of this thesis was to characterize a forelimb median nerve injury model using functional and histological metrics that will be used for future studies to elucidate the ErbB family role in nerve regeneration in transgenic mice (Chapter 4).

These research objectives were investigated using experiments organized around two separate aims involving *in vivo* and *in vitro* models of nerve regeneration.

Aim 1. Does lapatinib promote nerve regeneration in a mouse model of sciatic nerve injury?

This aim compared peripheral nerve regeneration in a mouse sciatic nerve transection and repair model between animals treated with lapatinib and vehicle controls. The extent of nerve regeneration was evaluated using retrograde labelling and nerve histomorphometry. Retrograde labelling assessed the number of motor and sensory neurons that regenerated 10 mm into the tibial nerve at 10 or 28 days after sciatic nerve injury and repair. Nerve histomorphometry assessed the number of myelinated axons, myelin thickness, fiber diameter and g-ratio in the tibial nerve at 10 or 28 days after sciatic nerve injury and repair, compared between groups. We **hypothesized** that treatment with lapatinib would enhance regeneration by increasing the number of myelinated axons and labelled sensory and motor neurons.

Aim 2. Does lapatinib or gefitinib promote neurite outgrowth in cultured dorsal root ganglion neurons in the presence of chondroitin sulfate proteoglycan?

In this aim, the mechanism by which ErbB inhibitors act was investigated using neurite outgrowth assays. The ability of lapatinib and gefitinib to rescue the neurite growth inhibiting effects of chondroitin sulfate proteoglycan (CSPG) on cultured DRG neurons was evaluated by

measuring neurite elongation. We **hypothesized** that lapatinib or gefitinib would rescue the inhibition of neurite growth that occurs with CSPG.

Chapter 2: Literature Review

2.1 Nerve anatomy

Like all systems of the human body, the nervous system is composed of cells that collectively form tissues, and tissues that form organs. At a cellular level, nervous tissue is formed by neurons and glia. Structurally, the nervous system is divided into the central nervous system (CNS) and the peripheral nervous system (PNS). Functionally, the nervous system can also be divided into the autonomic nervous system (ANS) and the somatic nervous system. The CNS is composed of the brain and spinal cord and contains a distinct population of glia that includes astrocytes, oligodendrocytes, microglia and ependymal cells. The PNS is composed of nerves and ganglia. It contains two types of glia, Schwann cells and satellite cells. The PNS, with a focus on nerves will now be explored further.

Peripheral nerves (hereafter referred to as ‘nerves’) along with ganglia, form the majority of the PNS and connect the CNS to sensory receptors in the skin and muscle. A nerve is a bundle of myelinated and unmyelinated axons in the PNS. There are 12 pairs of cranial nerves and 31 pairs of spinal nerves. Notably, the optic nerve (CN II) is not part of the PNS since it is derived from an outgrowth of the diencephalon and its axons are myelinated by oligodendrocytes instead of Schwann cells.⁷ A nerve is composed of axons and Schwann cells along with connective tissue, that will now be reviewed.

2.1.1 Axons and Schwann cells

Peripheral axons are elongated processes from a neuron cell body that innervate distal motor or sensory end organs. An axon is composed of both a cell membrane (axolemma) and cytoplasm (axoplasm). The functional unit of nerves are myelinated and unmyelinated axons that are surrounded by myelinating and non-myelinating Schwann cells, respectively. Several non-

myelinated axons are ensheathed by a non-myelinating Schwann cell forming what is termed a Remak bundle.⁸ For uninjured myelinated axons, there is a 1:1 relationship between a myelinating Schwann cell and its axon. Along a myelinated axon's length, it is surrounded by numerous myelinating Schwann cells which produces an insulating multilayered, myelin sheath composed of numerous lipids.⁹

The regions of a myelinated axon can be separated into repeating anatomically and functionally distinct domains called the node of Ranvier, paranode, juxtaparanode and internode (see Figure 2.1).¹⁰ The node of Ranvier was first described by the French histologist Louis-Antoine Ranvier in 1878. It is the 0.8-1.1 μm region where the axolemma is exposed between adjacent Schwann cells.¹⁰ At the node of Ranvier, voltage-gated sodium channels are clustered in the axolemma allowing for the saltatory conduction of action potentials.¹¹ Other proteins found at the node of Ranvier include neuronal cell adhesion molecule (NrCAM), neurofascin-186 and the actin-binding protein spectrin βIV .¹⁰ While mostly exposed, the node of Ranvier is also in contact with microvilli from the outer collar of Schwann cell cytoplasm. Interestingly, the diameter of the nodal axon is usually significantly smaller than that of the internodal axon, especially in large axons.¹² The paranode is the region adjacent to the node of Ranvier where the paranodal loops of Schwann cell cytoplasm are connected to the axon by septate-like junctions that involve caspr-1 and neurofascin 155.^{13,14} This axo-glial connection prevents diffusion between the periaxonal spaces of the node of Ranvier and juxtaparanode. The juxtaparanode is the region of an axon near a node of Ranvier, between the paranode and internode.¹² It contains delayed-rectifier potassium channels (Kv1.1, Kv1.2) and caspr-2.¹² The internode is the region of an axon between juxtaparanodes where the Schwann cell's myelin sheath provides electrical insulation. The Schwann cell nucleus is usually located near the middle of an internode where

Axons can be classified not only by their presence of myelin, but also by their diameter and conduction velocity into group A, group B or group C.¹⁶ Group A axons are the largest in diameter, fastest conducting and correspond to most somatic sensory axons and all motor axons. Group A axons can be further subdivided into type A α (70-120 m/s), A β (30-70 m/s) and A δ (12-30 m/s).¹⁶ Group B axons are smaller than group A and correspond to preganglionic autonomic axons. Group C are the smallest and slowest conducting axons being the only group that are unmyelinated. They correspond to postganglionic autonomic axons and somatic sensory axons for pain and temperature sensation. Nociceptive neurons which respond to pain have relatively small diameter axons, being classified as A δ or C. Alternatively, another classification system limits group A to somatic motor axons and classifies sensory axons as type I (large myelinated), type II (intermediate myelinated), type III (small myelinated) and type IV (unmyelinated).¹⁷

As axons travel within a nerve, they don't take a linear path, rather they undulate back and forth. This undulating pattern of axons forms visual transverse and oblique bands on the surface of the nerve that are visible with the naked eye or more easily with a surgical microscope. These bands were first described by the Italian scientist Felice Fontana in 1781 and were thus termed 'bands of Fontana'.^{18,19} Fontana also identified that this undulating pattern could explain a nerve's ability to accommodate stretching.¹⁹ Over the following hundreds of years there was controversy as to whether the bands of Fontana was actually caused by undulating axons or was based on the arrangement of nerve connective tissue.^{20,21} In 2018, Alvey et al. superimposed reflected light images with confocal images and conclusively showed that bands of Fontana are caused exclusively by undulating axons in a nerve.²²

2.1.2 Connective tissue layers

Nerves contain a significant amount of connective tissue that organizes the axons within. The connective tissue is divided into three layers from inner to outer named the endoneurium, perineurium and epineurium (see Figure 2.2). The endoneurium is composed of a matrix of type I and III collagen fibers that forms the intrafascicular connective tissue.²³ The term endoneurial channels is often used to describe the tunnels of endoneurium within which the axons and Schwann cells are located. The internal surface of the endoneurium is in direct contact with a continuous basal lamina which is produced by the Schwann cells within. The perineurium organizes a nerve into discrete fascicles and is composed of type I collagen, and layers of flattened polygonal cells called perineurial cells which form the blood-nerve barrier for the endoneurium, axons and Schwann cells within. The epineurium can be divided into an outer (external) epineurium forming the outermost protective layer and an inner (internal) epineurium between fascicles.²⁴ The epineurium contains fibroblasts, type I and III collagen as well as elastin fibers.^{25,26} This meshwork of fibers allows the nerve to accommodate some stretching and provides protection for the fragile axon within. The epineurium forms between 30-75% of the cross-sectional area of a nerve, and is especially prevalent in multifascicular nerves.²⁷ Proximally, a nerve is usually unifascicular and becomes multifascicular as it nears its target. As a nerve travels distally and becomes multifascicular, the nerve develops a consistent fascicular arrangement, termed the internal topography.²⁸ This consistency has allowed for nerve surgeons to develop surgical techniques that involve internal neurolysis to dissect out specific fascicles and coapt them to a denervated recipient nerve, termed a 'nerve transfer'. Surrounding the outer epineurium of a nerve is loose connective tissue called the mesoneurium which contains the segmental blood supply that enters a nerve to become the vasa nervorum. The connective tissue

layers of nerves are also innervated by nervi nervorum through free nerve endings throughout and Pacinian corpuscles in the endoneurium.⁷

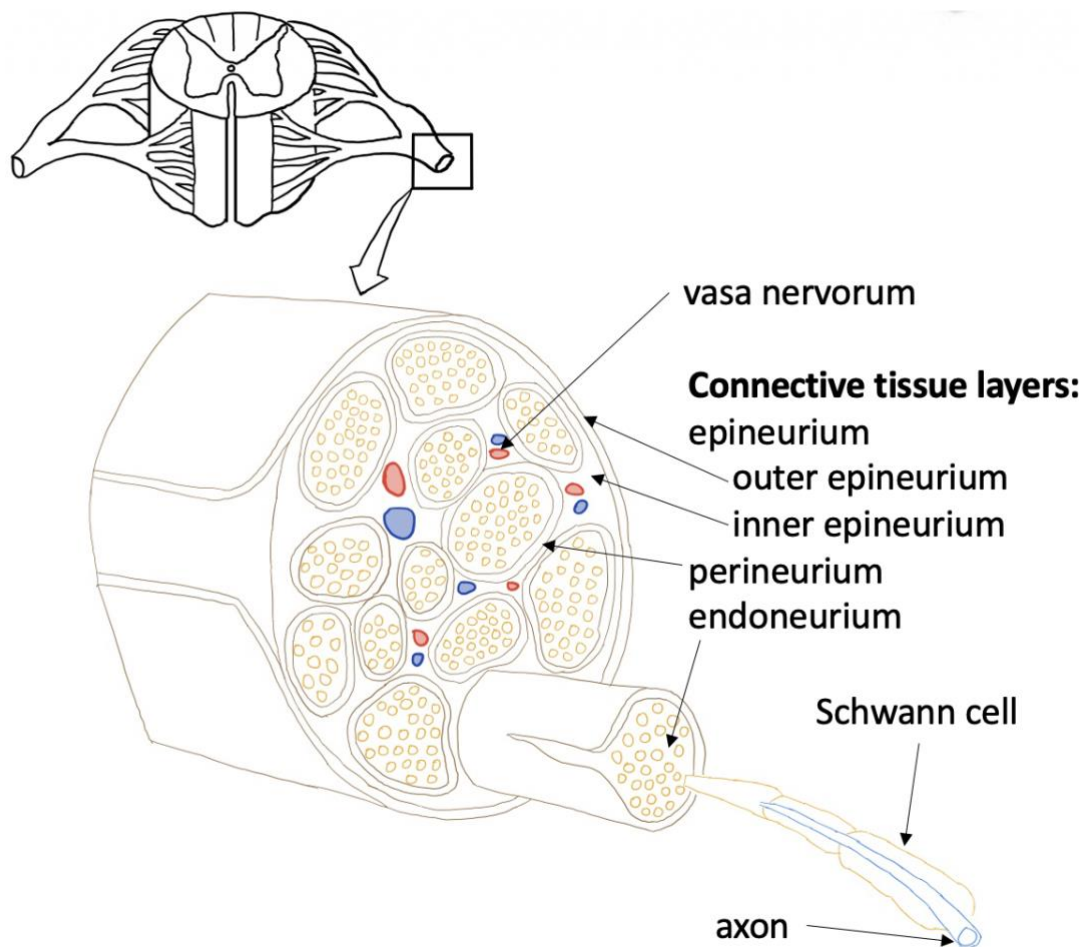


Figure 2.2 Nerve histology. A nerve is a bundle of axons in the PNS, and contains three layers of connective tissue, the endoneurium, perineurium and epineurium. The endoneurium surrounds an individual axons and associated Schwann cells. The perineurium surrounds a group of axons known as a fascicle. The epineurium can be divided into an inner epineurium between fascicles and an outer epineurium which surrounds the entire nerve. Image adapted by hand from *Peripheral nerve compression syndromes of the upper limb*.²⁹

2.2 Nerve injury

Nerve injury leads to substantial disability which considerably impacts on an individual's quality of life.³⁰ Following upper or lower limb trauma, the estimated incidence of nerve injury is 1.64%.⁵ Recovery of function following nerve injury is greatly influenced by the distance from the injury site to the target. The more proximal the injury, the fewer axons that can successfully elongate and form functional reconnections. The reduced success results from chronic denervation, chronic axotomy and denervation atrophy of targets.^{1,31} Nerve injury can be divided into different types based on the mechanism of the injury. The common mechanisms of injury are stretch, laceration, compression and mechanical deformation.³²

2.2.1 Classification of nerve injury

Nerve injuries are classified based on their severity to assist physicians in devising treatment plans and communicating prognoses to patients. Two nerve injury classification systems are used in clinical practice, the Seddon classification and the Sunderland classification (see Table 2.1 for comparison).

The Seddon classification was created by Herbert J. Seddon in 1942, with specific names suggested by Henry Cohen.^{33–35} Using the Seddon classification, a nerve injury is classified as neurapraxia, axonotmesis or neurotmesis. Neurapraxia is the mildest form of nerve injury in which there is damage to myelin but not axons, resulting in only a localized conduction deficit. Since there is no damage to axons, Wallerian degeneration (the breakdown of the distal segment of the transected axon; described in detail in Section 2.3) does not occur, and the injury usually completely resolves within 12 weeks. Neurapraxia is often caused by compression or ischemia. Axonotmesis describes a nerve injury in which there is damage to both myelin and axons, but the endoneurium, perineurium and epineurium remain partially or fully intact. Since there is damage

to axons, Wallerian degeneration occurs; however, since the endoneurium is preserved, functional recovery usually follows. Axonotmesis is often seen in crush and traction injuries. Neurotmesis is the most severe type of injury in which the nerve is completely transected. Without surgical intervention, no spontaneous recovery occurs because of nerve discontinuity and scar formation that prevents axon regeneration.³²

The Sunderland classification was created by Sydney Sunderland in 1951 and elaborated on the classification by Seddon, creating five degrees of nerve injury.³⁶ While first-degree and fifth-degree are identical to neurapraxia and neurotmesis, respectively, Sunderland further categorized axonotmesis into second, third or fourth-degree. In second-degree injuries, axons are damaged, but the endoneurium remains intact, allowing for the guidance of regenerating axons to their original target. In third-degree injuries, axons and the endoneurium are damaged, with only the perineurium and epineurium intact. Without the presence of endoneurial channels that guide regenerating axons to their original target, there is disordered regeneration that is further inhibited by scar tissue at the injury site. In fourth-degree injuries, there is damage to the perineurium resulting in significant scar formation at the injury site known as a neuroma-in-continuity. These injuries have very limited expectation of spontaneous recovery without neuroma excision and nerve grafting. A sixth-degree classification has also been added to describe the heterogeneity of injury pattern often encountered in ‘real-world’ context, where multiple degrees of injury can be found in the same injured nerve.^{37,38}

Table 2.1: Classification of nerve injury

Sunderland classification	Seddon classification	Parts of the nerve injured
First-degree	Neurapraxia	Myelin sheaths
Second-degree	Axonotmesis	Myelin sheaths and axons
Third-degree	Axonotmesis	Myelin sheaths, axons and endoneurium
Fourth-degree	Axonotmesis	Myelin sheaths, axons, endoneurium and perineurium
Fifth-degree	Neurotmesis	Myelin sheaths, axons, endoneurium, perineurium and epineurium

2.3 Nerve regeneration

Unlike axons in the CNS, axons in the PNS have a greater ability to regenerate because of the more growth supportive environment that exists following injury. When an axon is transected (termed axotomy), a neuron is split into two cellular components. The proximal part of the axon, which is still attached to the cell body, has the potential to regenerate. However, the distal component of the axon is separated from its cell body and will undergo anterograde degeneration which was first described by the English physician Augustus Waller in 1850 and is thus termed Wallerian degeneration.³⁹ Wallerian degeneration encompasses axonal and myelin degeneration, Schwann cell de-differentiation and proliferation. The mechanisms of Wallerian degeneration have been widely studied in the *Wld^S* mouse in which a chance spontaneous mutation in C57Bl/6 mice resulted in significantly delayed Wallerian degeneration.⁴⁰ It was later shown that increased expression of an enzyme in the nicotinamide adenine dinucleotide pathway was responsible for axonal protection that delayed Wallerian degeneration in these mice.⁴¹ The process of Wallerian degeneration and subsequent nerve regeneration will be reviewed by focusing on the response in the neuron and the role of Schwann cells and neurotrophic factors.

2.3.1 Response of the neuron

The closer the neuron cell body is to the axotomy, the more likely cell death will occur.⁴² Injury very close to the neuron cell body, such as in brachial plexus root avulsion injuries, eliminates the potential for nerve regeneration.⁴³ Within six hours of axotomy the neuron cell body responds through a process called chromatolysis (also called the “neuron reaction”). During chromatolysis, the nucleus is displaced from its central location to the periphery, the nucleolus enlarges and the rough endoplasmic reticulum (Nissl bodies) disperse.⁴⁴ As the neuron reaction occurs in the cell body, the axon also undergoes degenerative changes. Within two days following axotomy, the endoplasmic reticulum fragments, neurofilaments and microtubules disintegrate and mitochondria swell.⁴⁵ As the axon degenerates, it fragments and is phagocytosed by Schwann cells and invading macrophages. Interestingly the response of a neuron to axotomy differs depending on the setting of a previous nerve injury.⁴⁶ This response has been termed the conditioning effect and was first theorized to occur following the clinical observation that the rate of nerve regeneration was increased following a delayed repair compared to an immediate repair. A variety of conditioning lesions have been found to increase the rate of nerve regeneration including crush, vibration,⁴⁷ pulsed electromagnetic fields,⁴⁸ local inflammation⁴⁹ and compression.⁵⁰ The discovery of the conditioning effect resulted in significant interest in the identification of cellular and molecular changes that were improving the intrinsic growth state of the neuron. In the early 2000’s one of the multiple pathways that results in neuron conditioning was discovered.⁵¹ In conditioned DRG neurons it was revealed that increased cyclic adenosine monophosphate (cAMP) activates protein kinase A (PKA) which then phosphorylates the transcription factor cAMP response element-binding protein (CREB), resulting in the activation of numerous gene pathways that increase nerve regeneration. cAMP also increases the

production of growth-associated protein-43 (GAP-43) by activation of the transcription factor STAT3.⁵² Increased GAP-43 expression, along with actin and tubulin, leads to the conversion of the neuron into a regenerating phenotype and the development of a growth cone at the tip of the regenerating axon. The growth cone (also present during embryonic development) guides the axon as it elongates towards its target through endoneurial channels. The role of the ErbB family in guiding this regeneration will be discussed further in section 2.8. Numerous regeneration-associated genes are also upregulated in the neuron after injury which facilitate it in transitioning to a regenerative state. Examples of regeneration associated genes include c-Jun,⁵³ activating transcription factor-3⁵⁴ and SRY-box containing gene 11.⁵⁵

2.3.2 Role of Schwann cells

Within 48 hours following nerve injury, denervated Schwann cells proliferate, de-differentiate and transition to a non-myelinating phenotype, similar to the embryonic phenotype of Schwann cells in developing nerves.^{56,57} Unlike Schwann cell proliferation during development, proliferation following injury is highly dependent on cyclin D1.^{58,59} As they proliferate, Schwann cells also de-differentiate from a myelinating phenotype to a regenerative phenotype. De-differentiation results in the Schwann cell downregulating proteins important in myelin formation, including myelin basic protein, myelin-associated glycoprotein and protein 0. This de-differentiation is thought to be mediated by the expression of the transcription factors cJun and Notch.⁶⁰ As part of Wallerian degeneration, denervated Schwann cells activate resident macrophages and recruit hematogenous macrophages to assist in the phagocytosis of axonal and myelin debris.⁶¹ To prepare for axonal regeneration, these Schwann cells line the now empty endoneurial channels to form regenerative conduits referred to as “bands of Büngner” that guide regenerating axons to their targets.⁶² The Schwann cells also secrete factors that guide

regenerating axons including nerve growth factor,⁶³ neural cell adhesion molecules⁶⁴ and cytokines of the interleukin family.⁶⁵ The use of autologous Schwann cells within a nerve conduit has been explored as a method to enhance nerve regeneration and found some success in animal models.⁶⁶

2.3.3 Role of neurotrophic factors

Neurotrophic factors are a family of proteins that support the growth, differentiation and survival of neurons.⁶⁷ The prototypical neurotrophic factor is nerve growth factor (NGF), which was discovered by Rita Levi-Montalcini and Stanley Cohen in 1956.⁶⁸ NGF, along with brain-derived neurotrophic factor (BDNF), neurotrophin-3 (NT-3) and neurotrophin-4 (NT-4) form a subgroup of neurotrophic factors termed neurotrophins.⁶⁹ Other neurotrophic factors include glial cell-line derived neurotrophic factor (GDNF) and ciliary neurotrophic factor (CNTF). All members of the neurotrophin family bind to p75 and to one or more of the Trk receptor tyrosine kinases. NGF binds to TrkA, BDNF and NT-4 bind to TrkB and NT-3 binds to TrkC.

Neurotrophic factors are also important in regulating myelination and regeneration.^{70,71} BDNF binding to p75 at low doses increases nerve regeneration, while NT-3 binding to TrkC and BDNF binding to p75 at high doses decreases regeneration.⁷¹ In addition, following nerve injury expression of BDNF, GDNF and p75 increases in the distal stump, while NT-3 expression decreases transiently.^{72,73} Following this discovery, the addition of GDNF at the nerve injury site was researched as a method to enhance regeneration.⁷⁴⁻⁷⁶ Despite the expression of neurotrophic factors that can support axonal regeneration, this upregulation is only transient since chronically denervated Schwann cells lose their ability to produce neurotrophic factors and promote axonal regeneration.¹

2.3.4 Role of time and distance

Initial estimates of regeneration speed focused on clinical observations of moving areas of paresthesia or by observing the difference in the time of reinnervation of two adjacent muscles.⁷⁷ Subsequent experiments have demonstrated that the rate of regeneration depends on the species, injury and type of axon. In the human clinical domain, nerve regeneration is commonly referred to as occurring at a rate of 1 mm per day. Once an axon re-establishes connection with its target, the axon matures by enlarging in diameter and developing a myelin sheath.⁷⁸ The success of nerve regeneration following injury is highly dependent on the time it takes for regenerating axons to reach their target. Chronic axotomy, in which there is prolonged loss of contact between an axon and its target decreases the likelihood that functional recovery will occur.³¹ Furthermore, chronic denervation of both Schwann cells, which is the loss of contact between Schwann cells in the denervated distal stump and their axons, decreases their receptiveness to support functional reinnervation.⁷⁹ While it was originally thought that chronic muscle denervation was the most important factor that limited nerve regeneration, it is now understood that chronic axotomy and chronic denervation are the greatest limiters of success.³¹

2.3.5 Inhibitors of nerve regeneration

The success of nerve regeneration following injury is not only dependent on the intrinsic growth state of the neuron but also on growth supportive and inhibitory environmental cues that impact axonal regeneration.^{80,81} In both the CNS and the PNS, numerous molecules have been identified as having an inhibitory role in axonal regeneration.⁸¹

In the CNS, a glial scar produced at the injury site prevents regeneration across it. The glial scar is predominantly composed of reactive astrocytes. These astrocytes produce molecules that inhibit regeneration including keratan sulfate proteoglycans and chondroitin sulfate

proteoglycans (CSPG). Three CNS myelin proteins – myelin associated glycoprotein (MAG), Nogo-A and oligodendrocyte myelin glycoprotein, also inhibit axonal regeneration and are present within a glial scar.⁸² These myelin proteins all bind to the Nogo receptor which, with p75 and Lingo-1, activate intracellular signalling cascades that inhibit axonal regeneration.^{83,84}

In the PNS, there is a more permissive growth environment that allows for axonal regeneration as compared to the CNS. However, within the PNS exist some of the same inhibitors that exist in the CNS, such as CSPG. CSPGs are a family of extracellular proteins covered in sulfated glycosaminoglycans.⁸⁵ These include aggrecan, versican, neurocan and brevican which are produced by neurons and glia.⁸⁶ Following nerve injury, CSPG is upregulated and accumulates at the injury site, inhibiting axonal regeneration.⁸⁷ The mechanism by which CSPG inhibits axonal regeneration is thought to involve multiple pathways. Initially, it was thought the CSPG non-specifically blocks the binding of matrix molecules to cell surface receptors.⁸⁸ Subsequent studies have also shown that binding of CSPG to the leukocyte common antigen related phosphatase subfamily, protein tyrosine σ allows for its inhibitory effects.⁸⁹ CSPGs can be deactivated by the bacterial glycosaminoglycanase chondroitinase ABC and studies that have injected this enzyme into the nerve repair site have found an increase in the number of regenerating axons in the distal stump four days following injury.⁹⁰⁻⁹² Finally, CSPG may also activate ErbB1⁶ which will be described in section 2.7 on the role of the ErbB family in nerve regeneration.

2.4 Treatment of nerve injury

Treatment of nerve injury is primarily based on surgical strategies through nerve repair, nerve grafting, and nerve transfer combined with physical therapy. Nerve repair is the process in which the distal stump of a transected nerve is sutured to the proximal stump. Unfortunately,

following nerve injury there is often a significant gap between the nerve stumps that does not allow for a tensionless coaptation. In setting of a significant nerve gap an autologous nerve graft is often used to bridge the gap between the injured proximal and distal nerve stumps. However, in the setting of a substantial gap, and a more proximal injury, nerve transfer has emerged as a revolutionary strategy to improve functional recovery following nerve injury. Nerve transfer will now be explored further.

2.4.1 Nerve transfer

Over the past two decades, nerve transfer has emerged as a promising technique to support both motor and sensory reinnervation.⁹³⁻⁹⁵ Surgically, nerve transfer involves suturing a transected non-critical healthy ‘donor’ nerve to a more important injured ‘recipient’ nerve closer to the target of reinnervation. The donor nerve is transected as distally as possible, while the recipient is transected proximal to allow for a tensionless coaptation. The success of nerve transfer relies heavily on the time to target reinnervation and on the number of axons reaching the target.

Multiple nerve transfer coaptations have been developed based on the orientation of the donor and recipient nerves, including end-to-end, end-to-side and supercharged end-to-side (SETS) (see Figure 2.3). The choice of coaptation varies depending on the extent of the injury and the likelihood of native regeneration. The most common coaptation is the end-to-end, in which the proximal stump of the donor nerve is sutured to the distal stump of the injured nerve. The end-to-side nerve transfer was reintroduced by Viterbo in 1992.⁹⁶ It has also been referred to as the terminolateral nerve transfer. In an end-to-side coaptation, the distal stump of the injured recipient nerve is sutured to the side of a donor nerve, which acts as a source of collaterally sprouting axons. Unfortunately, while sensory axons undergo collateral sprouting, motor axons

only sprout following injury, requiring a proximal injury to the donor nerve if any motor sprouting is to be expected.⁹⁷ The end-to-side coaptation has fallen out of use in favour of the end-to-end and SETS coaptations. The SETS coaptation can be seen as a combination of the end-to-end and end-to-side coaptations. In this coaptation, a donor nerve is transected and sutured to the side of the injured recipient nerve through an epineurial or perineurial window.

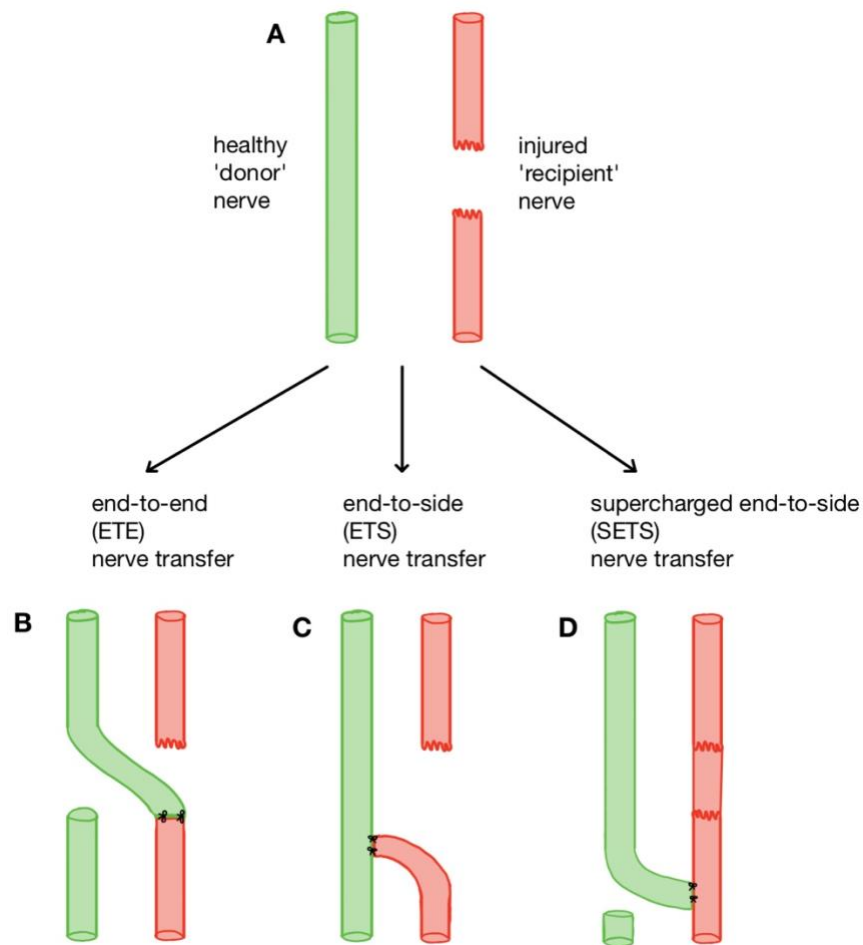


Figure 2.3 Nerve transfer coaptations. (A) An injured ‘recipient’ nerve (red) adjacent to a healthy ‘donor’ nerve (green). (B) In end-to-end (ETE) nerve transfer, the donor nerve is sutured end-to-end with the recipient nerve. (C) In end-to side (ETS) nerve transfer, the distal stump of the recipient nerve is sutured to the side of the donor nerve. (D) In supercharged end-to-side (SETS) nerve transfer, the proximal stump of the donor nerve is sutured to the side of the injured nerve near the target.

Many examples of nerve transfers have been proposed and performed for a variety of nerve injuries, and in recent years, spinal cord injury.⁹⁸ A common nerve transfer employed using the SETS coaptation is for proximal ulnar nerve injuries. This coaptation is used instead of an end-to-end transfer when the possibility of regeneration across the ulnar nerve injury site remains. In the transfer the pronator quadratus branch of the anterior interosseous nerve is transferred to the side of the ulnar motor nerve for the restoration of intrinsic muscle function. The transfer has no donor morbidity and successfully restores function to intrinsic muscles.⁹⁹ In recent years it has also found use in the treatment of severe cubital tunnel syndrome.^{100,101}

2.6 ErbB family

The ErbB (EGFR) family is a group of four homologous receptor tyrosine kinases named ErbB1, ErbB2, ErbB3 and ErbB4. Each receptor is composed of a glycosylated extracellular region, hydrophobic transmembrane segment and an intracellular domain composed of a juxtamembrane segment, intracellular protein kinase domain and a carboxyterminal tail with tyrosine phosphorylation sites.¹⁰² The extracellular region is composed of four highly conserved domains (I-IV).¹⁰³ Domains I and III facilitate ligand binding while cystine-rich domains II and IV allow for receptor dimerization. When ligand is not present, a binding loop of domain II is buried within a pocket of domain IV forming a closed conformation that is stabilized by hydrogen bonds and prevents receptor dimerization.¹⁰⁴ Signalling within the ErbB family follows a similar sequence of steps. Ligand binding triggers a conformational change that exposes the binding loop of domain II allowing for receptor dimerization.¹⁰⁵ Following dimerization, the intracellular protein kinase domain is activated resulting in the autophosphorylation of tyrosine residues and the stimulation of intracellular signalling cascades involved in cell survival, proliferation and adhesion.¹⁰⁶ The ‘lateral’ communication provided by receptor dimerization

allows for a greater number of responses than possible if only vertical signal transmission was possible. The ErbB family is named after the avian erythroblastosis virus in which an aberrant form of ErbB1 was found.¹⁰⁷ 11 ligands are able to bind to members of the ErbB family, including epidermal growth factor (EGF), transforming growth factor alpha (TGF- α), amphiregulin, betacellulin, epiregulin and the neuregulins (NRG).¹⁰⁶ The ErbB family has been especially implicated in the pathogenesis of cancer, and because of this numerous inhibitors have been developed and approved for various cancers. See Table 2.2 for an overview of each receptor.

Table 2.2 Overview of the ErbB family

ErbB family	Other names	Ligands
ErbB1	EGFR, HER1	EGF, TGF- α , HB-EGF, amphiregulin, betacellulin, epiregulin, epigen
ErbB2	HER2, neu, CD340	prolidase ¹⁰⁸
ErbB3	HER3	NRG1, NRG2, heregulin
ErbB4	HER4	neuregulins (1 α , 1 β , 2 α , 2 β), betacellulin, epiregulin, HB-EGF

2.6.1 ErbB1

ErbB1 is also known as epidermal growth factor receptor (EGFR). Seven ligands bind to ErbB1 including EGF, TGF- α , HB-EGF, amphiregulin, betacellulin, epiregulin, and epigen.¹⁰⁹ ErbB1 often forms a heterodimer with ErbB2 which amplifies the effect of ErbB1 signalling.¹¹⁰ Signalling via ErbB1 is important in organogenesis and oncogenesis.¹¹¹

2.6.2 ErbB2

ErbB2 (HER2, neu or CD340) was previously thought to be an orphan receptor and signal exclusively as a heterodimer, however recent work demonstrates prolidase as a high-affinity ligand.¹⁰⁸ With that said, the function of ErbB2 is thought to be as the preferred

dimerization partner with other members of the ErbB family that amplifies signal transduction, especially with ErbB3.^{110,112} Unlike the other ErbB receptors, ErbB2 is not dependent on ligand binding for dimerization since its extracellular domains I and III are fused together permanently exposing the binding loop of domain II.¹¹³ Despite the binding loop being constitutively exposed, ErbB2 homodimers are only seen in the presence of overexpression, since electrostatic repulsion prevents homodimerization.^{113,114} ErbB2 is strongly implicated in the pathogenesis of solid cancers such as 20-30% of breast cancers, in which it is associated with a poor prognosis.¹¹⁵

2.6.3 ErbB3

ErbB3 (HER3) is unique since it lacks a functional tyrosine kinase domain and is thus dependent on the formation of heterodimers with other members of its family.¹¹⁶ Since it lacks a kinase domain, theoretical ErbB3 homodimers would not be able to participate in signal transduction. Within the ErbB family, the ErbB2-ErbB3 heterodimer is the strongest signaller of cell growth.¹¹⁰ ErbB3 is able to bind neuregulin 1-2 and heregulin, and when dimerized with ErbB2 the affinity for neuregulin is increased.¹¹⁰ Binding of neuregulin-1 to the ErbB2-ErbB3 heterodimer is incredibly important in the regulation of Schwann development and in nerve regeneration.¹¹⁷

2.6.4 ErbB4

Like ErbB1, ErbB4 (HER4) is a classical receptor tyrosine kinase able to bind ligands and autophosphorylate via its kinase domain. ErbB4 has seven identified ligands including neuregulins 1-4, betacellulin, epiregulin and HB-EGF.¹¹⁸ ErbB4 primarily signals by forming heterodimers with ErbB2, though it can also form dimers with itself, ErbB1 and ErbB3. Signalling via ErbB4 is important in the development of the heart, neural crest and mammary

glands.¹¹⁹ ErbB4 knockout mice die by embryonic day 11 because of defective heart development.¹²⁰

2.7 ErbB inhibitors

ErbB tyrosine kinase inhibitors were developed following the discovery that the ErbB family plays a role in the pathogenesis of many cancers.¹⁰⁶ Following this, an effort was made to identify molecules which could inhibit these oncogenic pathways by binding to the ErbB family. In 1990 Fendly et al. screened numerous monoclonal antibodies for their ability to bind to ErbB1 or ErbB2.¹²¹ They identified six anti-ErbB1 antibodies and 10 anti-ErbB2 antibodies that each bound to a specific epitope of the extracellular regions of the receptors. The antibodies that bound the 4D5 and 2C4 epitopes were further developed into the drugs trastuzumab and pertuzumab, respectively. In the succeeding years, numerous types of ErbB inhibitors were developed, which can be classified based on the receptor they inhibit and structurally as a monoclonal antibody or small molecule. ErbB1 inhibitors include monoclonal antibodies cetuximab and panitumumab, as well as small molecule inhibitors gefitinib, erlotinib, afatinib. ErbB2 inhibitors include the therapeutic monoclonal antibodies trastuzumab, pertuzumab. Lapatinib is a dual small molecule inhibitor of ErbB1 and ErbB2. Trastuzumab, lapatinib and gefitinib will be described in more detail because of their past and present investigation in promoting nerve regeneration.

2.7.1 Trastuzumab

Trastuzumab (trade name Herceptin) is a humanized IgG1-kappa monoclonal antibody that binds to the 4D5 epitope of the extracellular domain IV of the ErbB2 receptor.^{121,122} In 1989, it was shown that the murine precursor to trastuzumab had a strong inhibitory effect on the growth of cultured breast cancer cells.¹²³ Cells that overexpress HER2 (ErbB2) undergo

antibody-dependent cellular cytotoxicity in the presence of trastuzumab, thus preventing their proliferation.¹²⁴ Other mechanisms by which trastuzumab may also inhibit ErbB2 signalling includes the promotion of internalization and subsequent degradation of membrane bound ErbB2 and inhibition of the PI3K pathway.¹²⁴ Clinically, trastuzumab was approved by the FDA in 1998, and is used in the treatment of HER2+ breast cancer where it reduces mortality and delays disease progression.^{125,126} In patients treated intravenously with trastuzumab there is a moderate risk of cardiotoxicity which in some cases can lead to heart failure.¹²⁷

2.7.2 Lapatinib

Lapatinib (trade name Tykerb) is a small molecule dual reversible inhibitor of ErbB1 and ErbB2. It was approved by the FDA in 2007, as an additional option for combination therapy in the treatment of advanced and metastatic HER2+ breast cancer.^{128,129} Unlike trastuzumab, it is taken orally as lapatinib ditosylate. Being a small molecule inhibitor, lapatinib can pass through the cell membrane and selectively inhibit the intracellular kinase domains of ErbB1 and ErbB2 preventing the activation of downstream second messengers.¹³⁰

2.7.3 Gefitinib

Gefitinib (trade name Iressa) is a substituted anilinoquinazoline small molecule selective inhibitor of ErbB1. Gefitinib competes with ATP for the tyrosine kinase domain of ErbB1 inhibiting autophosphorylation which prevents signal transduction.¹³¹ Clinically, it is indicated for the treatment of advanced non-small cell lung cancer with ErbB1 activating mutations.¹³²

2.8 Role of ErbB family in nerve regeneration

The ErbB family is involved in numerous signalling pathways in nervous system development and nerve injury that may promote or inhibit nerve regeneration. ErbB family receptors are expressed throughout the PNS, including sensory and motor neurons and Schwann

cells.¹³³ The most elucidated role of the ErbB family is in Schwann cells which strongly express ErbB2 and ErbB3.^{2,134} Neuregulin signalling through the ErbB2-ErbB3 heterodimer stimulates Schwann cell proliferation, migration and differentiation to promote nerve regeneration following injury.^{2,135} This heterodimer formation is important since ErbB2 is unable to bind neuregulins and ErbB3 has no kinase activity and thus must rely on ErbB2 for signalling. ErbB3 knockout mice have a significantly decreased number of Schwann cells, demonstrating the importance of ErbB3 in the differentiation and survival of Schwann cells.¹³⁶ When ErbB2 is absent, Schwann cells are present but their myelin sheaths are reduced in thickness.¹³⁷ Axolemma-bound neuregulin-1 type III isoform is thought to be the ligand that regulates myelination by binding the ErbB2-ErbB3 heterodimer.¹³⁴ Studies in which neuregulin-1 expression was inhibited have demonstrated a decrease in myelination and rate of regeneration following nerve injury.^{138,139} Similarly, neuregulin-1 overexpression causes hypermyelination, demonstrating the importance of it and its receptor pair in regulating myelin thickness. However, other studies have found that in adult mice which were prevented from expressing ErbB2 specifically in Schwann cells, there was no impact on the myelination of regenerating axons following nerve injury.¹⁴⁰

Following nerve injury, the expression profile of the ErbB family is altered in comparison to uninjured nerves. In a rat model of nerve injury it was found that ErbB1 and ErbB4 were downregulated, ErbB3 upregulated and ErbB2 expression did not change in the injured sciatic nerve.¹⁴¹ Overall, this demonstrates a dynamic response of the ErbB family following nerve injury.

A less elucidated but important role of the ErbB family in nerve regeneration involves ErbB1 signalling. In 2005, Koprovcica et al. showed that in the CNS, inhibitory substrates

including myelin proteins and CSPG activate ErbB1 through a calcium-dependant pathway to inhibit axonal regeneration.⁶ In the experiment, cultured cerebellar granule cells were immobilized on an inhibitory substrate and several small molecules were added to characterize their effect on neurite growth.⁶ Several ErbB1 kinase inhibitors were found to rescue the inhibitory effects of the substrate and promote neurite growth.⁶ In an optic nerve injury model, treatment with an ErbB1 inhibitor was also found to increase the number of regenerated axons 0.25 mm from the injury site compared to control.⁶ The ability of ErbB1 to inhibit axonal regeneration may also explain why ErbB1 expression is downregulated by approximately 50% following nerve injury.¹⁴¹ However, other studies have found that instead of acting through directly through ErbB1, ErbB1 inhibitors may promote neurite outgrowth by stimulating the secretion of neurotrophic factors by glia and neurons which then act in a paracrine or autocrine fashion.^{142,143} A follow-up study using ErbB1 knockout mice instead found that as previously thought, ErbB1 inhibitors act directly through ErbB1 receptors to promote axonal regeneration.¹⁴⁴

Following the discovery that the ErbB family has numerous roles in the repair of the nervous system, the FDA approved ErbB2 inhibitor trastuzumab was investigated for its ability to regulate both acute and chronic nerve regeneration.^{3,145} Paradoxically, it initially was observed that trastuzumab increased the number of regenerating axons after immediate nerve repair in the rat sciatic nerve injury model.¹⁴⁵ 4 weeks following acute nerve injury and repair, there were significantly more myelinated axons in the common peroneal nerve 10 mm from the repair site, in mice treated with trastuzumab than with control.³ However this pro-regenerative effect was only observed in acutely and not chronically axotomized motor neurons.³ In the proximal nerve stump the presence of phosphorylated ErbB1 was also found to be downregulated in trastuzumab-treated rats compared to controls. It was hypothesized that trastuzumab was able to

promote axonal regeneration by a newly identified mechanism independent of neuregulin signalling, by preventing signalling through the ErbB1-ErbB2 heterodimer.³ Overall, the regulatory impact of the ErbB family on nerve regeneration appears diverse with many areas remaining to be investigated. The therapeutic potential of small molecule inhibitors of ErbB1 and ErbB2 warrants further investigation and is the subject of this thesis.

Chapter 3: Inhibition of the ErbB1 and ErbB2 receptors increases the number of regenerating myelinated axons in a mouse model of nerve injury

3.1 Introduction

Nerve injury is a common clinical challenge that has considerable impact on an individual's quality of life and function.^{5,30,146} Unfortunately, there are currently no approved non-surgical treatments that directly increase the rate of nerve regeneration and improve functional recovery. Chronic axotomy and chronic Schwann cell denervation combined with long regenerative distances result in poor functional outcomes following nerve injury.^{31,79} The ErbB family is involved in both the promotion and inhibition of nerve regeneration. The most elucidated role is in the ErbB2-ErbB3 heterodimer which binds neuregulin-1 and promotes Schwann cell de-differentiation, proliferation and migration following injury.^{2,135} However, it has been paradoxically observed that inhibition of the ErbB2 receptor by the monoclonal antibody trastuzumab increased the number of regenerating myelinated axons in a rat sciatic nerve injury model.³ Furthermore, phosphorylated ErbB1 levels were found to be downregulated in the distal stump of the injured nerve.³ These findings led to the hypothesis that trastuzumab disrupts an inhibitory dimerization between ErbB1 and ErbB2. This hypothesis was also informed by priorly demonstrating that activated ErbB1 signalling inhibits axonal regeneration following activation by chondroitin sulfate proteoglycan (CSPG).⁶ Furthermore, use of an ErbB1 inhibitor was found to rescue the inhibitory effect of CSPG on axonal regeneration.⁶ Despite this, it is still unknown how inhibition of ErbB1 and ErbB2 impacts the success of nerve regeneration.

The primary aim of this study was to evaluate how ErbB1-ErbB2 inhibition using lapatinib or solo ErbB1 inhibition using gefitinib could affect nerve regeneration *in vivo* and *in vitro* model of nerve injury. Lapatinib is a dual ErbB1-ErbB2 tyrosine kinase inhibitor currently

used in the combination treatment of HER2+ breast cancer.¹²⁸⁻¹³⁰ We hypothesized that preventing the dimerization of the ErbB1-ErbB2 heterodimer using lapatinib would promote nerve regeneration. This hypothesis was tested using a sciatic nerve transection and immediate repair mouse model, followed by retrograde labelling and nerve histomorphometry to evaluate regenerative success. Furthermore, neurite growth assays were performed to evaluate how neurite length differs between lapatinib and gefitinib when in the presence of the axonal regeneration inhibitor CSPG. The repurposing of currently approved therapeutics to enhance nerve regeneration could one day improve the rate of functional recovery following nerve injury.

3.2 Methods

3.2.1 Experimental design and animal numbers

To investigate the impact on regeneration by lapatinib, 24 male, 25-week-old C57Bl/6 mice were divided into a 10-day or 28-day cohort each containing treatment and control group. On day 0 all mice underwent hindlimb surgery for right sciatic nerve transection and repair. From day 0 until the 10- or 28-day endpoint, mice were administered lapatinib or vehicle via oral gavage in the treatment and control groups, respectively. Outcomes measured at both time points were the number of regenerated sensory and motor neurons through retrograde labelling. For the group with a 28-day endpoint, nerve histomorphometry was performed to determine the number of regenerating myelinated axons, fiber diameter and g ratio.

Animal cages were housed in a temperature and humidity-controlled room with 12-hour light/dark cycles. Animals were fed with standard chow and water *ad libitum*. All animal procedures were approved by the Queen's University Animal Care Committee, in accordance with the guidelines set forth by the Canadian Council on Animal Care.

Table 3.1 Summary of experiment groups and animal numbers in lapatinib nerve regeneration experiment.

Timepoint	Treatment	Animal Numbers
10-day	lapatinib	6
	vehicle	6
28-day	lapatinib	6
	vehicle	6

3.2.2 Lapatinib and vehicle administration

For the administration lapatinib, a 100 mg/kg suspension was created in 0.5% hypromellose and 0.1% of Tween 80 in sterile water as described in Gustafson, 2013.¹⁴⁷ The concentration of lapatinib was chosen based on studies that evaluated the permeability of lapatinib to brain tumors across the blood-brain barrier, which may best model restricted delivery across the blood-nerve barrier.^{148–150} Mice were individually weighed and 0.1 mg/g of lapatinib was administered via oral gavage daily until the 10- or 28-day endpoint.

3.2.3 Surgical procedures

All surgical procedures were performed with aseptic technique and the use of an operating microscope (Leica Microsystems). Mice were induced into general anesthesia via inhaled isoflurane and maintained under a sufficient plane of anesthesia titrated to respiratory rate. The mouse was positioned prone, the limbs secured to the table and the right hindlimb shaved and sterilized with povidone iodine from the greater trochanter to the knee joint. The line from the palpable greater trochanter to the knee joint was used as a reference point. 2 mm below this line and parallel to it, an incision was made to expose a plane between the biceps femoris and vastus lateralis. Upon retraction of the biceps femoris the sciatic nerve was visualized which distally bifurcated into the tibial and common peroneal nerves. After identifying the sciatic nerve, it was transected immediately distal from its emergence beneath the gluteal muscles using

micro-scissors and repaired using two 9-0 epineurial sutures. Following repair, the wound was irrigated and closed in layers.

Tibial nerve retrograde labelling

On day 10 or 28, the previous site of sciatic nerve repair containing epineurial sutures was identified and 10 mm distal to this site, the tibial nerve was transected using micro-scissors. A 1 mm segment of the distal tibial nerve stump was harvested for quantitative histomorphometry. Next, the proximal tibial nerve stump was submerged in a Vaseline well constructed on a parafilm base containing 10 μ L of Fluorogold (hydroxystilbamidine bis[methanesulfonate]; Sigma, St. Louis MO; #39286; 4% [wt./vol.]). After 1 hour, the well was removed, the wound irrigated and closed in layers. This process labels all sensory neurons in the lumbar DRG and motor neurons in the ventral horn of the lumbar spinal cord that regenerated their axons 10 mm into the tibial nerve following sciatic nerve transection and repair.

3.2.4 Retrograde labelled tissue: harvesting, processing and analysis

One week following retrograde labelling, mice were euthanized via intraperitoneal injection of sodium pentobarbital (32.5 mg/kg) and immediately perfused with 100 mL of 4% paraformaldehyde (PFA). Subsequently, the lumbar spinal cord and the L3/L4 dorsal root ganglia (DRG) were harvested and placed in 4% PFA. Tissue was cryoprotected in 4% PFA with 30% sucrose for 5 days and embedded in OCT medium (Tissue-Tek; Andwin Scientific, Woodland Hills, CA) and sectioned using a cryostat. The lumbar spinal cord was sectioned coronally at 50 μ m, while the DRG were sectioned at 25 μ m. Using a fluorescent microscope, the number of motor and sensory neurons in the spinal cord and DRG, respectively were counted with the slides blinded. The counted raw total was corrected by multiplying it by a correction factor described

by Abercrombie, based on the diameter of 20 neuron cell bodies and the section thickness to reach the corrected total.¹⁵¹

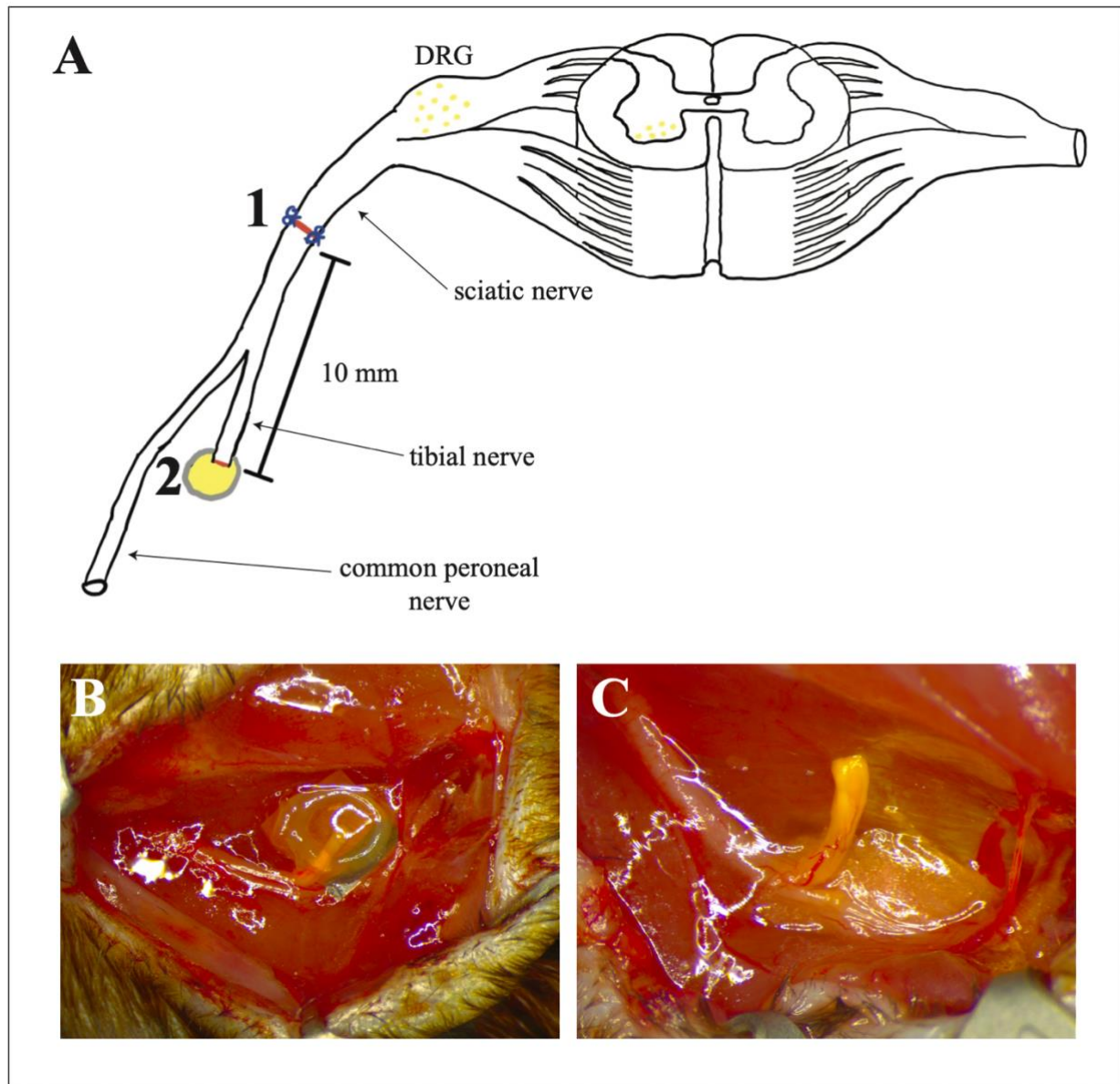


Figure 3.1 Surgical techniques. (A1) Diagrammatic representation of surgical procedures. The right sciatic nerve was transected immediately distal to its emergence beneath the gluteal muscles (red line) and repaired using two 9-0 epineurial sutures (blue). (A2) 10 mm distal to the repair site on day 10 or 28, the tibial nerve was transected (red line) and retrogradely labelled using Fluorogold (yellow). Fluorogold labels sensory neurons in the DRG and motor neurons in the ventral horn of the spinal cord that regenerate into the tibial nerve. A 1 mm segment of the tibial nerve was harvested immediately distal the site of retrograde labelling for nerve histomorphometry (B) Surgical image of proximal stump of tibial nerve exposed to Fluorogold within a petroleum jelly well. (C) 1 hour following retrograde labelling, the proximal stump of the tibial nerve was visibly labelled.

3.2.5 Nerve histomorphometry

For each mouse, a 1 mm segment of the right tibial nerve was harvested 10 mm distal to the sciatic nerve repair site and placed in 2.5% glutaraldehyde at 4°C for 2 days. The nerves were then postfixed in 1% osmium tetroxide, serial methanol dehydrated, embedded in Jembed 812 resin (Canemco. Inc., Montréal, Québec) and cross-sectioned at 1.5 µm using an ultramicrotome (RMC Products, Tucson, AZ). For each tibial nerve segment, from each animal, a cross-section was imaged at 100x magnification using NeuroLucida software (MBF Bioscience, Williston, VT). The number of myelinated axons, average axon diameter, average fiber diameter and average g-ratio were measured using a semi-automated custom program in MATLAB (MathWorks Inc, Natick, MA).¹⁵²

3.2.6 Neurite outgrowth assay

To investigate the mechanisms responsible for the effects of ErbB1 inhibition on sensory and motor neurons following nerve injury, we carried out neurite outgrowth assays. In these assays, we tested the *in vitro* effects of ErbB inhibitors lapatinib and gefitinib on DRG neurite outgrowth exposed to the inhibitor chondroitin sulfate proteoglycan (CSPG). DRGs from the cervical, thoracic and lumbar spinal cord were harvested as according to Sleigh et al, 2016.¹⁵³ DRG neurons were dissociated, cultured for 48 hours in Neurobasal A complete medium and divided into six groups depending on the presence of an ErbB inhibitor, CSPG or both. Six exposure groups were compared including control, CSPG alone (200 ng/mL), lapatinib alone (10 µmol/L), gefitinib alone (10 µmol/L), CSPG + lapatinib and CSPG + gefitinib. Concentrations of the ErbB inhibitors lapatinib and gefitinib were chosen based on previous concentrations found to be active in studies of lapatinib distribution across the blood-brain barrier to HER2+ brain metastases and *in vitro* assays.¹⁴⁸ The ability of lapatinib and other small mol Each plate was

immunostained for beta-tubulin to provide visualization of the entire neuron including its neurites. From each plate a representative number of neurons were imaged with a high-resolution scanning digital camera mounted on a fluorescent microscope (Carl Zeiss Vision, München-Hallbergmoos, Germany). AxioVision software (version 4.2) was used to capture 48-bit RGB color images at 1300x1300 pixels. Images were then adjusted for brightness and contrast in Photoshop (Adobe Systems, San Jose, CA) to ensure all neurites were visible. Finally, the length of the longest neurite from its origin at the neuron cell body to its tip was measured using the semi-automated neurite tracing program NeuronJ.¹⁵⁴

3.2.7 Statistical analysis

The number of retrogradely-labelled neurons and nerve histomorphometry parameters between the lapatinib and vehicle groups were statistically compared using one-tailed unpaired *t*-tests. An alpha of 0.05 was used in all statistical analyses and significance was defined as $p < 0.05$. Mean and standard error of the mean were calculated and presented. The mean length of the longest neurite in neurite outgrowth assays with or without the presence of an ErbB inhibitor and/or CSPG were statistically compared using one-way ANOVA.

3.3 Results

3.3.1 Animal survival

All surgeries and oral gavage administration of lapatinib and vehicle were tolerated well with two exceptions. A moderate amount of weight loss was observed in most animals and was theorized to be the result of the physical stress of the multiple surgeries and daily oral gavage. Two mice in the 28-day lapatinib group were euthanized on postoperative day 23 because of greater than 20% weight loss. Thus, these two mice were not retrogradely labelled and did not have a segment of their tibial nerve harvested for histomorphometry.

3.3.2 Lapatinib does not increase the number of regenerating sensory or motor neurons, 10- or 28-days following nerve repair

Retrograde labelling of the tibial nerve demonstrated positive labeling in the lumbar spinal cord and lumbar DRG. For the 10-day group the L4 DRG and lumbar spinal cords were blindly counted for the number of labelled sensory neurons. For the 28-day group, the L3/L4 DRG and lumbar spinal cords were counted. The number of regenerated sensory neurons did not differ significantly between lapatinib (222 ± 71) and vehicle (232 ± 52) at 10 days ($p > 0.05$), or between lapatinib (343 ± 69) and vehicle (499 ± 128) at 28 days ($p > 0.05$) (Figure 3.2 A-B). The number of regenerated motor neurons at 10 days did not differ significantly between mice treated with lapatinib (120 ± 43) compared to vehicle (84 ± 21) ($p > 0.05$). Similarly, the number of regenerated motor neurons at 28 days did not differ significantly between lapatinib (169 ± 30) compared to vehicle (128 ± 26) ($p > 0.05$) (Figure 3.2 C-D). As expected, following a longer time for regeneration, the number of regenerated sensory and motor neurons was significantly increased at 28 days compared to 10 days in both the lapatinib and vehicle groups ($p < 0.05$).

3.3.3 Lapatinib increases the number of regenerating myelinated axons following nerve repair

In the 28-day cohort a cross-section from the 1 mm segment of the right tibial nerve was analyzed histologically for the number of myelinated axons, average myelin thickness, fiber diameter and g-ratio (Figure 3.3). The number of myelinated axons in the tibial nerve was significantly higher in mice treated with lapatinib (1042 ± 108) compared to vehicle (729 ± 110 ; $p < 0.05$). However, no differences in average myelin thickness, fiber diameter or g-ratio were observed between lapatinib and vehicle groups ($p < 0.05$). Nerve histomorphometry analysis was

not performed in the 10-day group because of excessive axonal and myelin debris, and limited remyelination that prevents analysis of regenerating myelinated axons.¹⁵⁵

3.3.4 Gefitinib promotes neurite extension in cultured DRG neurons

The effect of lapatinib and gefitinib in the axonal regeneration inhibitor was evaluated using *in vitro* neurite growth assays to evaluate neurite growth. CSPG is a known inhibitor of axonal regeneration, which in cultured neurons inhibits the formation of neurites. Measurement of the longest neurite for each cultured DRG neuron demonstrated differences in the average neurite length depending on the presence of CSPG or the ErbB inhibitors lapatinib and gefitinib (Figure 3.4). The mean length of the longest neurite was significantly greater in DRG cultures containing an ErbB inhibitor in the presence of CSPG (lapatinib: $85.9 \pm 21.0 \mu\text{m}$; $p < 0.01$, gefitinib: $277 \pm 26.5 \mu\text{m}$; $p < 0.0001$) than CSPG alone ($23.6 \pm 5.0 \mu\text{m}$). However, in DRG cultures containing only lapatinib, the mean longest neurite was significantly decreased ($74.4 \pm 27.4 \mu\text{m}$) compared to control ($294 \pm 21.3 \mu\text{m}$; $p < 0.0001$). This indicates a possible neurotoxic effect of lapatinib at this concentration that while possibly preventing some CSPG-mediated inhibition, prevents normal growth. Furthermore, interference of cell adherence to the plate could have prevented normal growth. Dose titrations of lapatinib are currently being performed to assess whether different concentrations may alleviate this neurotoxic effect.

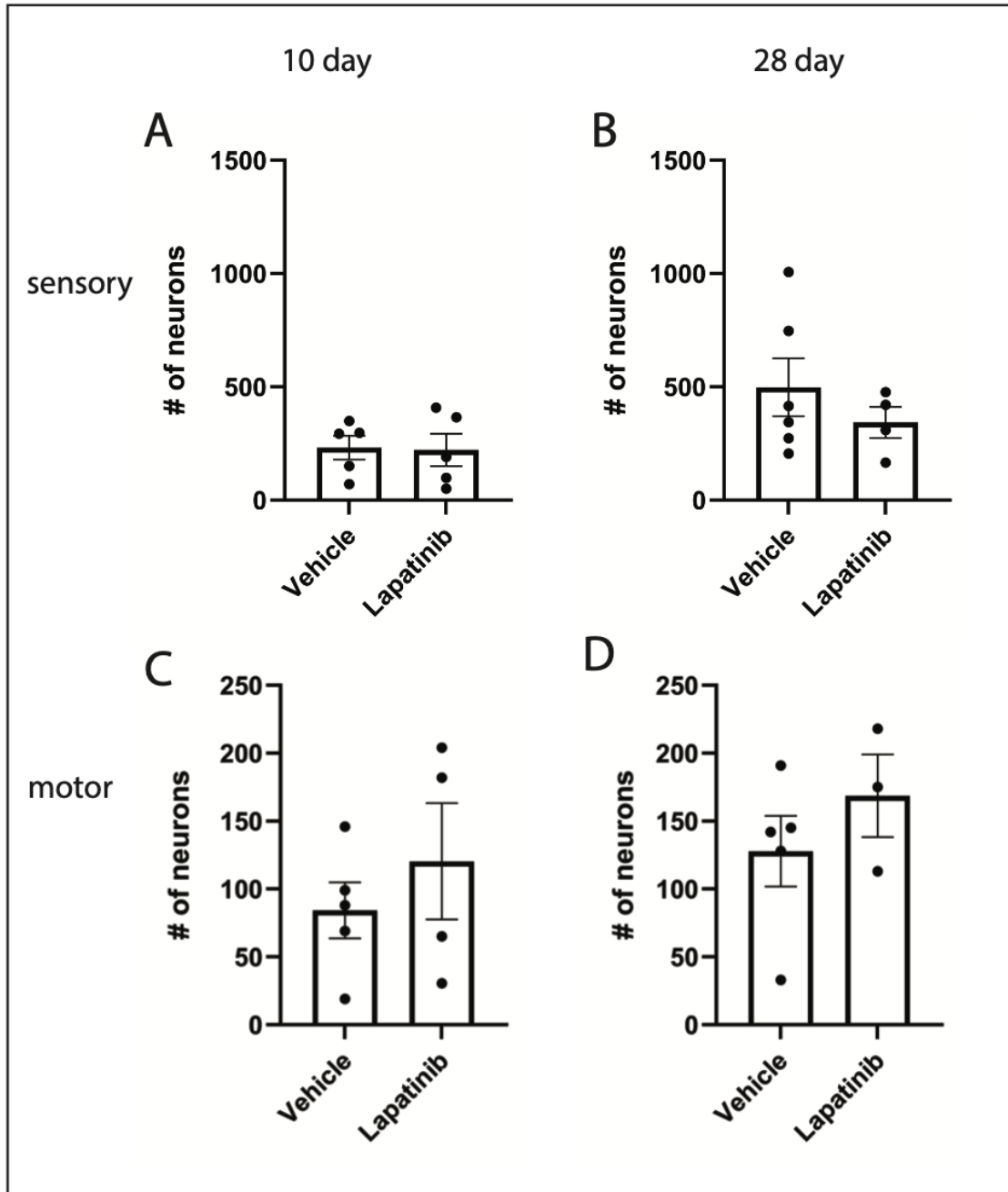


Figure 3.2 The number of regenerated sensory or motor neurons following sciatic nerve transection is not statistically different between lapatinib and vehicle treated mice.

Retrograde labelling of regenerated motor and sensory neurons of the tibial nerve, following sciatic nerve transection and repair, did not show enhancement of nerve regeneration by lapatinib. (A-B) No difference in the number of regenerated sensory neurons in lumbar DRG was observed in the lapatinib treated mice compared to vehicle. (C-D) Similarly, no difference in the number of retrogradely labelled regenerated motor neurons in the spinal cord was observed in the lapatinib treated mice compared to vehicle. A greater number of motor neurons was identified at 28-days in both groups, compared with 10 days, as would be expected. Error bars represent standard error of the mean.

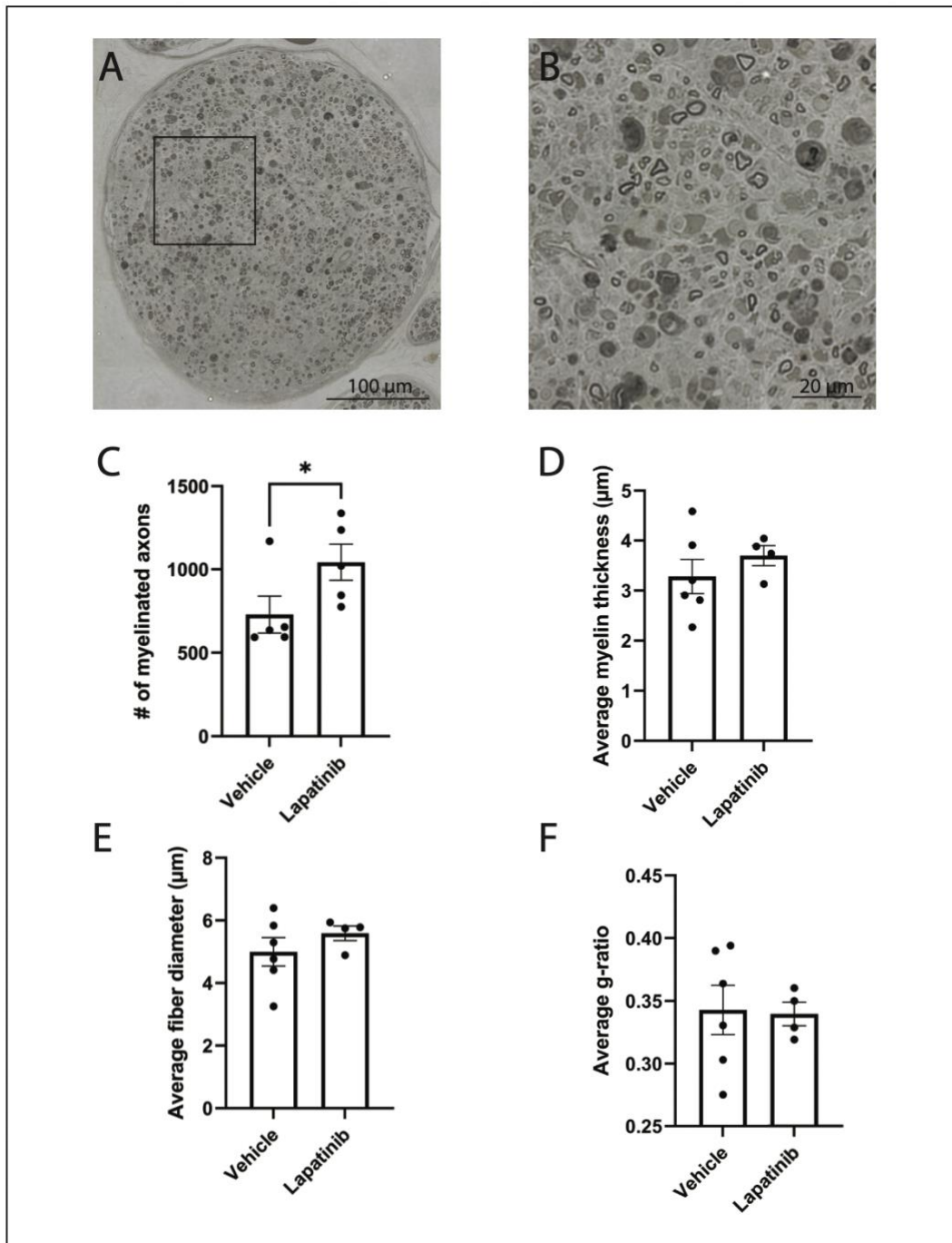


Figure 3.3 Administration of lapatinib increases the number of regenerated myelinated axons 28 days following nerve repair. (A) Representative cross-section of a tibial nerve postfixed with osmium tetroxide in a mouse 28 days following sciatic nerve transection and repair treated with lapatinib. (B) Zoomed in region from A showing myelinated axons which were quantitatively assessed in each nerve for the number of myelinated axons (C), average myelin thickness (D), average fiber diameter (E) and average g-ratio (F). The number of regenerated myelinated axons was significantly increased in lapatinib treated mice.

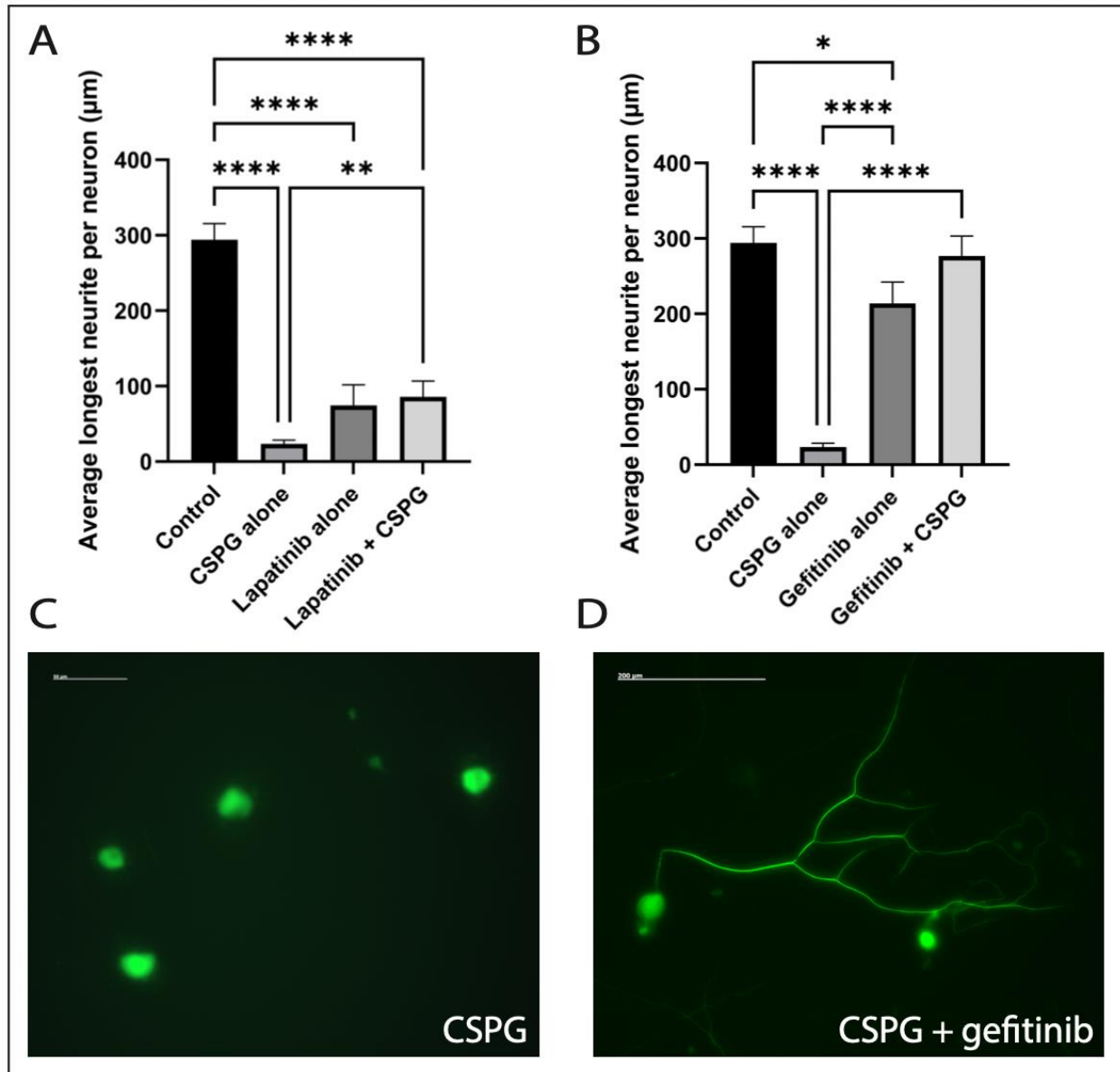


Figure 3.4 Gefitinib rescues the effect of CSPG mediated neurite growth inhibition.

(A) Average neurite length compared between six cell cultures plated with the axonal regeneration inhibitor CSPG and/or an ErbB inhibitor. Both gefitinib and lapatinib were able to rescue some of the inhibitory effect of CSPG on neurite growth inhibition. However, compared to control cultures lapatinib may have also had a neurotoxic effect. (B) The presence of the ErbB1 inhibitor gefitinib with CSPG significantly increased the average length of the longest neurite compared to cell cultures that contained only CSPG. (C-D) Representative cell culture images of DRG neurons immunostained for beta-tubulin plated with CSPG (C) or CSPG and gefitinib (D), demonstrating a rescue of CSPG mediated neurite growth inhibition. Error bars represent standard error of the mean. Scale bars: 50 µm (C) and 200 µm (D). Mean neurite length was statistically compared using one-way ANOVA in both A and B ($p < 0.05$: *, $p < 0.01$: **, $p < 0.001$: ***, $p < 0.0001$: ****).

3.4 Discussion

This study used both *in vivo* and *in vitro* models to evaluate the ability of lapatinib and gefitinib to promote nerve regeneration. This study did not find an increase in the number of regenerated motor or sensory neurons as was found in prior studies using the ErbB2 inhibitor trastuzumab in a rat model.³ Retrograde labelling of sensory and motor neurons that regenerated into the tibial nerve demonstrated significant variance within and between groups that likely confounded interpretation of the results (see Figure 3.2). This variance could have been caused by multiple factors including variable staining intensity with Fluorogold, lost tissue during sectioning and fascicular misalignment during nerve repair that could have directed neurons of interest variably into the tibial or common peroneal nerve. Quantitative analysis of the tibial nerve revealed a greater number of regenerated myelinated axons in mice treated with lapatinib (see Figure 3.3). This finding is consistent with previous studies in which the ErbB2 inhibitor trastuzumab was found to increase the number of regenerated myelinated axons in a rat model of nerve injury.^{3,145}

The mechanism by which ErbB1-ErbB2 inhibition facilitates regeneration is believed to occur separate from the neuregulin-1 pathway and involving a potential inhibitory dimerization between ErbB1 and ErbB2.³ In a previous study, activated ErbB1 was significantly decreased in the proximal stump of the transected common peroneal nerve in rats treated with trastuzumab.³ It had been suggested that the mechanism by which ErbB1 inhibition promotes axonal regeneration is through off target effects,¹⁴³ however follow up studies using a ErbB1 conditional knockout model disputed this theory.¹⁴⁴ Furthermore, CSPG, a known inhibitor of axonal regeneration, has been shown to activate ErbB1, which may explain the ability of ErbB inhibitors to promote nerve regeneration.⁶ In contrast to the neuregulin-1 ErbB2-ErbB3 signalling pathway, CSPG mediated

activation of the ErbB1-ErbB2 heterodimer may function as an axonal stop signal during growth. We hypothesize that this signal may be vital during normal development of the peripheral nervous system but following nerve injury in which regeneration inhibitors are especially prevalent at the injury site, this signalling pathway may prevent more robust axonal growth. This hypothesis is supported by the finding that while the number of regenerated neurons was not significantly different, there were a greater number of regenerated myelinated axons which may suggest a role of Erb1-ErbB2 signalling in limiting axonal sprouting. Previous studies have similarly found that axonal regeneration is enhanced in retinal ganglion cell neurons following injury⁶ and that in *nrg-1* knock out mice there is increased axonal sprouting at the neuromuscular junction.¹³⁸ Axonal sprouting is the process by which myelinated axons form collateral branches at nodes of Ranvier. Sprouting occurs profusely following nerve injury and may function to protect from chronic Schwann cell denervation by filling the maximum number of endoneurial channels. Although lapatinib may have been able to increase axonal sprouting, this does not mean that functional recovery would have improved, and follow-up studies should include a functional metric of regenerative success. Analysis of the axon diameter distribution was unable to be completed because of software limitations. In rat, the normal axon diameter distribution of the tibial nerve is unimodal with a range of 2 – 12 μm and a peak at approximately 8 μm .¹⁵⁶ In the setting of nerve transection and repair, regenerating axons are of smaller diameter and have decreased myelin sheath thickness.³ The distribution of axon diameters of mice treated with lapatinib is not expected to differ significantly from vehicle, as in Hendry et al., 2016 in which there was no significant difference in the histograms of common peroneal nerves between the ErbB2 inhibitor trastuzumab and saline treated mice.

The inhibitory ErbB1-ErbB2 pathway was further elucidated in this study using neurite growth assays, in which it was unexpectedly shown that the ErbB1 inhibitor gefitinib has a stronger neurite growth promoting effect than the dual ErbB1-ErbB2 inhibitor lapatinib. This effect must be confirmed by follow-up assays which evaluate multiple titrations of both gefitinib and lapatinib to determine the ideal concentration that minimizes toxicity and enhances growth.

A major strength of this study is that it is the first to suggest and provide preliminary evidence for the mechanism by which ErbB inhibitors can promote histological regeneration following nerve injury. However, the gold-standard of evaluation of nerve regeneration is functional analysis and further studies must include this metric. This study is also limited in that it did not confirm that lapatinib administration was able to inhibit ErbB1 and ErbB2 signalling. In future studies, we will use a mouse median nerve model of nerve injury (described in Chapter 4) to evaluate how both systemic and local gefitinib administration effects histological and functional outcomes of nerve regeneration. The ability of gefitinib to adequately prevent phosphorylation of ErbB1 will also be confirmed through Western blot analysis.

The repurposing of an FDA approved molecular therapies like the ErbB inhibitors lapatinib or gefitinib has significant therapeutic potential and a more streamlined translation into the clinical realm. The market for peripheral nerve injuries is steadily increasing and impacts approximately 20 million people in the U.S. with nerve injuries each year and an associated \$20 billion cost to the U.S. healthcare system.^{4,5} This study provides additional evidence that the ErbB family can both promote or inhibit nerve regeneration depending on the receptors involved.

3.5 Conclusion

In conclusion, the dual ErbB1-ErbB2 inhibitor lapatinib increased the number of myelinated axons that regenerated into the tibial nerve as measured by nerve histomorphometry.

In vitro neurite growth assays demonstrated a neurite growth promoting effect of gefitinib that was stronger than lapatinib. Future studies should assess the nerve regeneration effects of the ErbB1 inhibitor gefitinib in an *in vivo* model. These experiments are in the preparatory stage and will be carried out in the summer of 2021.

Chapter 4: Characterization of a mouse forelimb model of median nerve injury

4.1 Introduction

The investigation of methods to enhance nerve regeneration and research nerve injury has led to the development of numerous animal models (for a review see Ronchi et al., 2019).¹⁵⁷ The choice of an experimental model is dependent on many factors. Important qualities of a rodent nerve injury model include the degree to which the structure and cellular regulation mimic the pathological state. These are often reflected in the structural dimensions of the nerve (length and diameter) and preserved cellular regulation within mammals. The cost of the animal and associated housing is also important from a practical standpoint. The rat sciatic nerve injury model is the most common *in vivo* model in nerve regeneration research. Rats are easy to house and have adequately-sized nerves that require less intensive microsurgical expertise compared to smaller species. Rats also have robustly characterized functional metrics validated for sciatic nerve injuries such as the sciatic functional index, tapered beam and walking track analysis.¹⁵⁸ While the sciatic nerve is chosen since it is the largest nerve in most species, in rodents, injury to the sciatic nerve results in paralysis of the hindlimb and joint contractures and automutilation behaviour that limits functional analysis.¹⁵⁹ These drawbacks to sciatic nerve injury have led to increased use of the median nerve as an injury model.^{157,160} Following median nerve transection, rodents are less likely to develop joint contractures and automutilate, which facilitates functional assessment by forelimb grip strength.^{161,162} While originally it was thought that the rat forelimb finger flexors were innervated by both the ulnar and median nerves,¹⁶³ Bertelli et. al, 1995 demonstrated that they are solely innervated by the median nerve.¹⁶⁰ Recovery of grip strength following median nerve transection is thus completely dependent on the success of median nerve

regeneration. Furthermore, the use of a forelimb model is also more clinically relevant since nerve injuries in humans occur more commonly in the upper limb. However, a limitation of any rat model is the availability of transgenic models for the investigation of molecular pathways that regulate nerve regeneration. The use of transgenic models allows for the knockout or over-expression of specific genes of interest to identify their role in nerve regeneration. While a rat transgenic model exists for the visualization of nerves through expression of Thy1-GFP,^{164,165} there are a limited number of models available to investigate molecular pathways associated with nerve regeneration. The use of mouse models in nerve regeneration research thus comes with both advantages and drawbacks. In this study we sought to characterize a mouse forelimb nerve injury model to determine uninjured median nerve histological and functional metrics. This model will be applied to the future investigation of ErbB signalling and ErbB inhibitors in nerve regeneration.

4.2 Methods

4.2.1 Experimental design and animal numbers

This experiment aimed to characterize the uninjured motor and sensory neuron pool as well as quantify the number and myelination parameters of axons within the proximal mouse median nerve. These baseline metrics will serve as a reference to interpret experimental nerve injury models in future work. To determine these uninjured parameters, six C57Bl/6 mice had their median nerve transected and retrograde labelled. A segment of the median nerve for quantitative histomorphometry was also harvested during this initial procedure. Seven days later, mice were perfused, the DRG and spinal cord harvested for labelled neuron counting and a segment of the median nerve harvested for nerve histomorphometry. Furthermore, baseline grip

strength measurements before and after median nerve transection were obtained to serve as a functional metric for nerve recovery.

Animal cages were housed in a temperature and humidity-controlled room with 12-hour light/dark cycles. Animals were fed with standard chow and water *ad libitum*. All animal procedures were approved by the Queen's University Animal Care Committee, in accordance with the guidelines set forth by the Canadian Council on Animal Care.

4.2.2 Retrograde labelling

All surgical procedures were performed with aseptic technique and the use of an operating microscope (Leica Microsystems). Mice were induced into general anesthesia via inhaled isoflurane and maintained under a sufficient plane of anesthesia titrated to respiratory rate. The mouse was positioned supine, the limbs secured to the table and the left forelimb was shaved from the axilla to the wrist. A longitudinal incision was created from the axilla to the elbow and the median nerve was identified travelling with the brachial artery and then circumferentially mobilized. The median nerve was then transected 3 mm proximal to the medial epicondyle of the humerus using micro-scissors. A 1 mm segment of the median nerve distal to this transection site was harvested for histomorphometry and fixed in 2.5% glutaraldehyde. Next, the proximal median nerve stump was submerged in a Vaseline well constructed on a parafilm base containing 5 μ L of Fluorogold (hydroxystilbamidine bis[methanesulfonate]; Sigma, St. Louis MO; #39286; 8% [wt./vol.]). After 1 hour, the well was removed, the wound irrigated and closed in layers.

4.2.3 Retrograde labelled tissue: harvesting, processing and analysis

One week following retrograde labelling, mice were euthanized via intraperitoneal injection of sodium pentobarbital (32.5 mg/kg) and immediately perfused with 100 mL of 4%

paraformaldehyde (PFA). The cervical spinal cord and the C5-T1 dorsal root ganglia (DRG) were then harvested and placed in 4% PFA. Tissue was cryoprotected in 4% PFA with 30% sucrose for 5 days and embedded in OCT medium (Tissue-Tek; Andwin Scientific, Woodland Hills, CA) and sectioned using a cryostat. The cervical spinal cord was sectioned coronally at 50 μm , while the DRG were sectioned at 25 μm . Using a fluorescent microscope, the number of motor and sensory neurons in the spinal cord and DRG, respectively, were counted. The raw total was corrected by multiplying it by a correction factor described by Abercrombie. This correction factor is based upon the diameter of 20 neuron cell bodies and the section thickness to reach the corrected total.¹⁵¹

4.2.4 Nerve histomorphometry

The 1 mm segment of the median nerve harvested at the time of retrograde labelling described above, was fixed in 2.5% glutaraldehyde at 4°C for 2 days. The nerves were then postfixed in 1% osmium tetroxide, serial methanol dehydrated, embedded in Jembed 812 resin (Canemco. Inc., Montréal, Québec) and cross-sectioned at 1.5 μm using an ultramicrotome (RMC Products, Tucson, Arizona). For each median nerve segment, an entire section was imaged at 100x magnification using Neurolucida software (MBF Bioscience). The number of myelinated axons, average myelin thickness, fiber diameter and g-ratio were measured using a semi-automated custom program in MATLAB (MathWorks, MA).¹⁵²

4.2.4 Forelimb grip strength

Forelimb grip strength was assessed in four mice, three days before median nerve transection for retrograde labeling and four days following, using a grip meter designed for rodents, Bioseb BIO-GS3 (Bioseb Pinellas Park, FL). Mice were held by the tail and allowed to grip onto a metal grid using only their forepaws. Slowly, the mouse was pulled by the tail

parallel to the axis of the grip meter. The grip meter recorded the largest resisted force, measured in grams that the mouse was able to generate with its grip before letting go. Each mouse was tested five times with two minutes of rest between trials, with the average of the five trials used. In the setting where the mouse lacked motivation to grip or did not properly grasp the grid, the trial was repeated.

4.3 Results

4.3.1 Mouse median nerve gross anatomy

The mouse median nerve was first characterized anatomically in perfused mice by meticulous dissection of the median nerve from origin in the brachial plexus to its entrance to the carpal tunnel in the wrist (Figure 4.1). The median nerve originated from the medial and lateral cords in the brachial plexus and traveled through the arm with the brachial artery and ulnar nerve. As the median nerve approached the cubital fossa, it diverged laterally from the ulnar nerve to enter the forearm. No branches of the median nerve were observed until it entered the forearm. Transection and repair of the median nerve was notably more technically challenging than the sciatic nerve repair described in Chapter 3, owing to the smaller diameter of the median nerve.

4.3.2 Quantification of the uninjured median nerve motor neuron pool

In the cervical spinal cord, retrograde labelling of the median nerve demonstrated a robust population of motor neurons in the ventral horn (Figure 4.1). The mean number of labelled motor neurons was 188 ± 9 . Motor neuron counts for one of the mice were not possible because of significant folding of tissue that obscured the labelled neurons. Sensory neuron counts are still pending at the time of thesis composition due to the challenges posed by sectioning these very fine structures which required outsourcing to a third party.

4.3.3 Median nerve histomorphometry

A cross-section from each median nerve was analyzed for the number of myelinated axons, average myelin thickness, fiber diameter and g-ratio (Figure 4.3). The mean number of myelinated axons was 1343 ± 109 , mean myelin thickness was $3.6 \pm 0.15 \mu\text{m}$, mean fiber diameter was $7.8 \pm 0.45 \mu\text{m}$, and mean g-ratio was 0.53 ± 0.01 .

4.3.4 Forelimb grip strength

Forelimb grip strength was assessed both prior to and following median nerve transection for retrograde labelling. Two mice were not evaluated for forelimb grip strength since they were initially used for a proof of principle that the retrograde labelling technique would enable visualization of the median nerve neuron pool. Following median nerve transection, it was observed that the affected forepaw had lost all ability to grip the metal grid and would consistently use a ‘paddling’ motion to use the injured forelimb. Through multiple trials over several days, it was observed that measured grip strength demonstrated some variation between mice and between trials of the same mouse. As expected, there was approximately a 50% reduction in normalized grip strength following median nerve transection. We also observe that grip strength values slightly increased as the animal recovered from surgery and likely began to use its uninjured forelimb more dominantly (Figure 4.4). Since there was no repair of the transected median nerve and the timepoint following surgery was short, no significant recovery from nerve regeneration would be plausible.

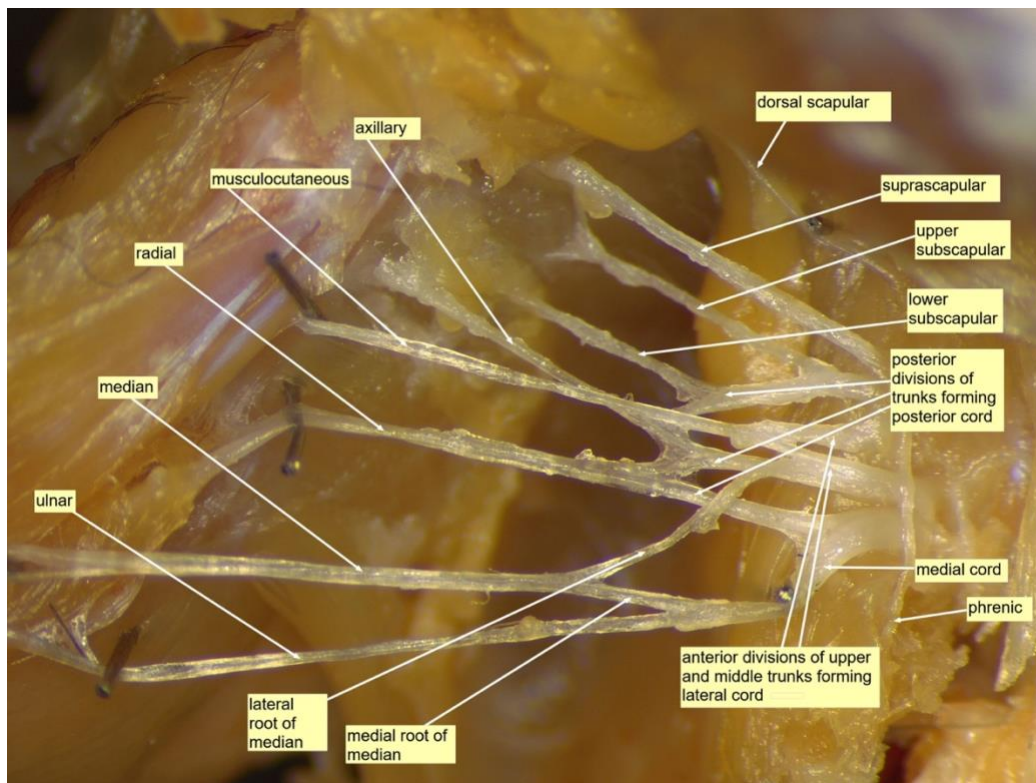


Figure 4.1 The mouse brachial plexus. Dissection of the mouse brachial plexus revealed a similar structure as in humans. The terminal branches are visible on the left and include the axillary, musculocutaneous, radial, median and ulnar nerves.

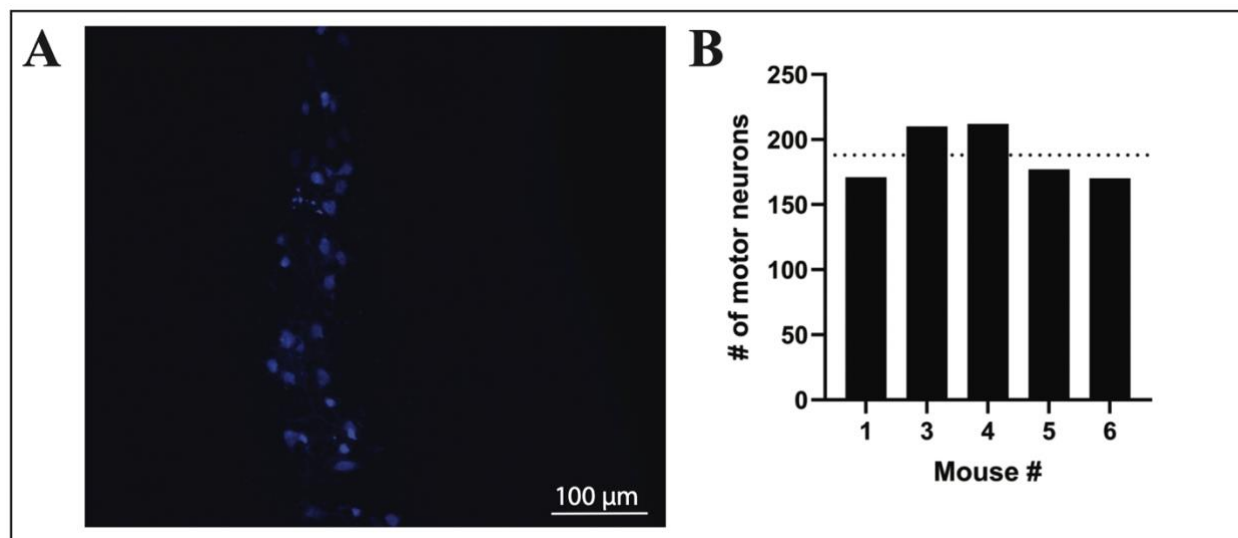


Figure 4.2 Retrograde labelled motor neurons of the median nerve. (A) Fluorogold labelled motor neurons of the median nerve are visible in the ventral horn of the cervical spinal cord. (B) The number of labelled motor neurons between each mouse median nerve was similar with a mean of 188. Mouse 2 spinal cord tissue was too folded to enable counting and was thus discarded.

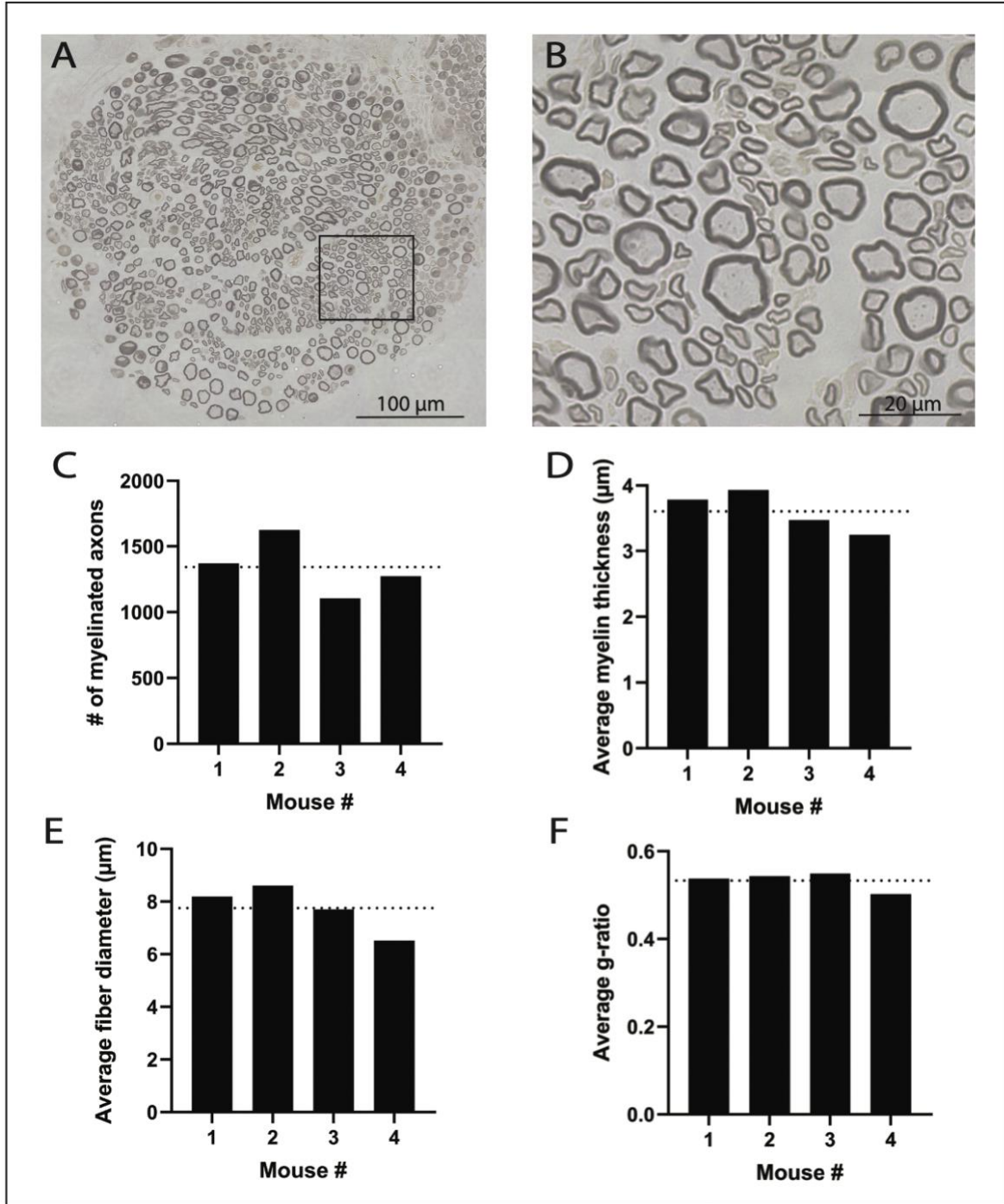


Figure 4.3 Median nerve histomorphometry. (A) Representative whole cross-section of a mouse median nerve postfixed with osmium tetroxide. (B) Zoomed in region from A showing myelinated axons which were quantitatively assessed in each median nerve for the number of myelinated axons (C), average myelin thickness (D), fiber diameter (E) and g-ratio (F). Most parameters were similar between mice, as expected in these uninjured nerves. The dotted horizontal line in C-F represents the mean.

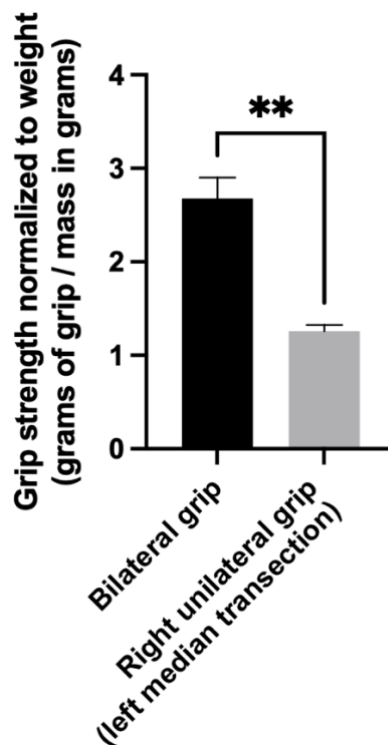


Figure 4.4 Forelimb grip strength following median nerve transection. Following left median nerve transection there was a significant decrease in forelimb grip strength ($p < 0.05$) because of paralysis of forepaw digit and wrist flexors.

4.4 Discussion

The use of a median nerve injury model in mice has numerous advantages over the common rat sciatic nerve injury model and allows for the investigation of recovery from nerve injury through functional and histological outcomes. Furthermore, the potential use of transgenic mice allows for the elucidation of molecular pathways that regulate nerve injury. Despite the differences between rat and mice models, all rodent models have notable limitations in their comparison to human nerve injuries because of the slower rate of nerve regeneration in humans and the longer regenerative distances.

This study defined baseline values for the assessment of functional and histological recovery in a mouse median nerve injury model. Nerve histomorphometry using semi-automated software was used to count the total number of myelinated axons, average myelin thickness, fiber

diameter and g-ratio. Interestingly, the number of myelinated axons counted was significantly less than counted through extrapolation via stereological principles by both light and electron microscopy in Jager et al., (2014).¹⁶⁶ The use of stereological principles has multiple limitations in the accurate counting and morphological analysis of regenerating axons.¹⁶⁷ Biological variation, particle misidentification and different sampling schemes can result in stereological estimates that are substantially different than would be determined through more exhaustive manual efforts.¹⁶⁷ Methods such as the ‘ratio technique’ which multiple axon density but nerve cross-sectional area have been advanced by fractionator techniques that help eliminate bias.¹⁶⁸ By counting each myelinated axon individually through the entire median nerve section, this study provided a more accurate reference value for the number of myelinated axons in the uninjured median nerve than can be estimated using stereological principles. Our estimates did not include unmyelinated axons, which would require electron microscopy or correlation with neurofilament-stained cross sections.¹⁶⁹ The mean myelinated axon number derived in this study may also be an underestimate given studies have demonstrated that use of transmission electron microscopy allows for the identification of more small myelinated axons than possible with light microscopy.¹⁶⁶ Interestingly, other histological parameters also differed from Jager et al., (2014), both average myelin thickness and fiber diameter were greater than previously found.¹⁶⁶ The ratio of the axonal diameter over the fiber diameter (g-ratio), was found to compare similarly to the commonly considered optimal g-ratio of 0.6.¹⁷⁰

Functional testing of forelimb grip strength following median nerve transection confirmed that grip strength in the injured forelimb had no observable role of the ulnar nerve. This finding aligns with previous studies that evaluated mouse and rat forelimb grip strength following median nerve injury.^{161,162} Grip strength was observed to decrease by 50% following

median nerve transection, in which the animal was now only able to grip with one forelimb. We did not assess the time for median nerve regeneration to allow for some recovery of grip, as this will be evaluated in longer-term studies of either median nerve transection and repair or crush injury.

This study has developed histological and functional metrics in a mouse model of median nerve injury that will allow for the comparison in other surgical and therapeutic techniques to enhance nerve regeneration using the mouse median nerve as a model. This model also avoids some of the pitfalls associated with the rat sciatic nerve that limit functional analysis of regeneration.¹⁵⁹ Furthermore, we believe that the use of transgenic mice with this forelimb model will enable for the further elucidation of the molecular mechanisms that regulate nerve regeneration following injury.¹⁵⁷ In our lab, future experiments will utilize this model for the preclinical investigation of the ErbB family and ErbB inhibitors in nerve regeneration.

4.5 Conclusion

In conclusion, the mouse median nerve injury model has several advantages over the rat sciatic nerve injury model. In this study the anatomy and histological features of the mouse median nerve were characterized which will serve as an uninjured comparison group in future forelimb median nerve injury studies.

Chapter 5: General discussion, conclusions, and future directions

The primary aim of this thesis was to evaluate the ability of the ErbB inhibitors lapatinib and gefitinib to promote nerve regeneration. We hypothesized that lapatinib, a dual ErbB1-ErbB2 inhibitor and gefitinib a sole ErbB1 inhibitor would promote nerve regeneration in *in vivo* and *in vitro* models. This hypothesis was supported by previous work demonstrating the role of ErbB1 signalling in inhibiting axonal regeneration,^{6,144} and the finding that ErbB inhibition by the monoclonal antibody trastuzumab could promote nerve regeneration in a rat model.¹⁴⁵ To test this hypothesis histological metrics of regeneration in a mouse sciatic nerve injury model were compared in mice treated with lapatinib or vehicle. Furthermore, the mechanism by which the ErbB inhibitors may promote nerve regeneration was explored using neurite outgrowth assays.

The number of regenerated sensory or motor neurons was not significantly different between mice treated with lapatinib compared to vehicle, however, there were a greater number of regenerated myelinated axons, which may suggest a role of Erb1-ErbB2 signalling in limiting axonal sprouting. The inhibitory ErbB1-ErbB2 pathway was further elucidated in this thesis using neurite outgrowth assays, in which it was unexpectedly shown that the ErbB1 inhibitor gefitinib had a stronger neurite growth promoting effect than the dual ErbB1-ErbB2 inhibitor lapatinib. This effect must be confirmed by follow-up assays which evaluate multiple titrations of both gefitinib and lapatinib to determine the ideal concentration that minimizes toxicity and enhances growth. Based on past studies^{6,144} and these present findings, it is suggested that CSPG-mediated activation of the ErbB1-ErbB2 heterodimer is a negative regulator of axon regeneration in both the CNS and PNS. Solo ErbB1 (gefitinib), ErbB2 (trastuzumab), or dual ErbB1-ErbB2 inhibition (lapatinib) is expected to promote axonal regeneration throughout the nervous system in *in vivo* and *in vitro models* by preventing the activation of this growth inhibitory pathway.

A major strength of this study is that it is the first to suggest and provide preliminary evidence for the mechanism by which ErbB inhibitors can promote histological regeneration following nerve injury. However, to translate these findings to clinical use, it is essential to determine if the effects of ErbB inhibition also promote functional recovery. This study is also limited in that it did not confirm that lapatinib administration was able to inhibit ErbB1 and ErbB2 signalling. In future studies, we will use a mouse median nerve model of nerve injury to evaluate how both systemic and local gefitinib administration affects histological and functional outcomes of nerve regeneration. The ability of gefitinib to adequately prevent phosphorylation of ErbB1 will also be confirmed through Western blot analysis. Furthermore, the dose-response relationship of lapatinib and gefitinib should be explored to determine the ideal concentration which limits neurotoxicity and promotes growth.

The repurposing of an FDA-approved molecular therapies like the ErbB inhibitors lapatinib or gefitinib has significant therapeutic potential and a more streamlined translation into the clinical realm. The market for peripheral nerve injuries is steadily increasing and impacts approximately 20 million people in the U.S. with nerve injuries each year and an associated \$20 billion cost to the U.S. healthcare system.^{4,5} This thesis provides additional evidence that the ErbB family can both promote or inhibit nerve regeneration depending on the receptors involved.

A secondary aim of this thesis was to characterize a mouse forelimb model of nerve injury for use in future experiments. Uninjured histological metrics of the mouse median nerve including the number of myelinated axons, mean axon diameter, mean myelin thickness and mean fiber diameter were determined. A functional metric of nerve regeneration using a forelimb grip strength meter was also characterized before and after transection of the median nerve.

This mouse model of median nerve injury that will allow for the comparison of other surgical and therapeutic techniques to enhance nerve regeneration using the mouse median nerve as a model. This model also avoids some of the pitfalls associated with the rat sciatic nerve that limit functional analysis of regeneration.¹⁵⁹ Furthermore, we believe that the use of transgenic mice with this forelimb model will enable for the further elucidation of the molecular mechanisms that regulate nerve regeneration following injury.¹⁵⁷ In our lab, future experiments will utilize this model for the preclinical investigation of the ErbB family and ErbB inhibitors in nerve regeneration.

References

1. Sulaiman, O. A. R. & Gordon, T. Role of chronic schwann cell denervation in poor functional recovery after nerve injuries and experimental strategies to combat it. *Neurosurgery* vol. 65 (2009).
2. Carroll, S. L., Miller, M. L., Frohnert, P. W., Kim, S. S. & Corbett, J. A. Expression of neuregulins and their putative receptors, ErbB2 and ErbB3, is induced during Wallerian degeneration. *J. Neurosci.* **17**, 1642–1659 (1997).
3. Hendry, J. M. *et al.* ErbB2 blockade with Herceptin (trastuzumab) enhances peripheral nerve regeneration after repair of acute or chronic peripheral nerve injury. *Ann. Neurol.* (2016) doi:10.1002/ana.24688.
4. Lundborg, G. Nerve injury and repair - A challenge to the plastic brain. in *Journal of the Peripheral Nervous System* vol. 8 209–226 (John Wiley & Sons, Ltd, 2003).
5. Taylor, C. A., Braza, D., Rice, J. B. & Dillingham, T. The incidence of peripheral nerve injury in extremity trauma. *Am. J. Phys. Med. Rehabil.* (2008) doi:10.1097/PHM.0b013e31815e6370.
6. Koprivica, V. *et al.* Neuroscience: EGFR activation mediates inhibition of axon regeneration by myelin and chondroitin sulfate proteoglycans. *Science (80-.)*. **310**, 106–110 (2005).
7. Standring, S. *Gray's Anatomy*. (Elsevier, 2015).
8. Harty, B. L. & Monk, K. R. Unwrapping the unappreciated: recent progress in Remak Schwann cell biology. *Current Opinion in Neurobiology* vol. 47 131–137 (2017).
9. Salzer, J. L. Schwann cell myelination. *Cold Spring Harb. Perspect. Biol.* **7**, (2015).
10. Buttermore, E. D., Thaxton, C. L. & Bhat, M. A. Organization and maintenance of molecular domains in myelinated axons. *Journal of Neuroscience Research* vol. 91 603–622 (2013).
11. Huxley, A. F. & Stampfli, A. R. *EVIDENCE FOR SALTATORY CONDUCTION IN PERIPHERAL MYELINATED NERVE FIBRES*. *J. Physiol. (1949)* vol. 8 <https://www.ncbi.nlm.nih.gov/pmc/articles/PMC1392492/> (1949).
12. Peles, E. & Salzer, J. L. Molecular domains of myelinated axons. *Current Opinion in Neurobiology* vol. 10 558–565 (2000).
13. Trapp, B. D. & Kidd, G. J. Axo-glial septate junctions: The maestro of nodal formation and myelination? *Journal of Cell Biology* vol. 150 97 (2000).
14. Menegoz, M. *et al.* Paranodin, a glycoprotein of neuronal paranodal membranes. *Neuron* **19**, 319–331 (1997).
15. Arroyo, E. J. & Scherer, S. S. On the molecular architecture of myelinated fibers. *Histochemistry and Cell Biology* vol. 113 1–18 (2000).
16. Brushart, T. M. *Nerve Repair*. (Oxford University Press, 2011).
17. Boyd, I. A. & Davey, M. R. *Composition of Peripheral Nerves*. (E & S Livingston).
18. Fontana, F. *Traité sur le vénin de la vipere sur les poisons americains, sur le laurier-cerise et sur quelques autres poisons végetaux* . ([s.n.], 1781).
19. Clarke, E. & Bearn, J. G. The spiral nerve bands of fontana. *Brain* **95**, 1–20 (1972).
20. Zachary, L. S., Dellon, E. S., Nicholas, E. M. & Dellon, A. L. The structural basis of Felice Fontana's spiral bands and their relationship to nerve injury. *J. Reconstr. Microsurg.* **9**, 131–138 (1993).
21. Merolli, A., Mingarelli, L. & Rocchi, L. A more detailed mechanism to explain the 'bands

- of Fontana' in peripheral nerves. *Muscle and Nerve* **46**, 540–547 (2012).
22. Alvey, L. M., Jones, J. F. X., Tobin-O'Brien, C. & Pickering, M. Bands of Fontana are caused exclusively by the sinusoidal path of axons in peripheral nerves and predict axon path; evidence from rodent nerves and physical models. *J. Anat.* **234**, 165–178 (2019).
 23. Lorimier, P. *et al.* Ultrastructural localization of the major components of the extracellular matrix in normal rat nerve. *J. Histochem. Cytochem.* **40**, 859–868 (1992).
 24. Millesi, H. & Terzis, J. K. Problems of terminology in peripheral nerve surgery: Committee report of the International Society of Reconstructive Microsurgery. *Microsurgery* **4**, 51–56 (1983).
 25. Salonen, V., Lehto, M., Vaheri, A., Aro, H. & Peltonen, J. Endoneurial fibrosis following nerve transection - An immunohistological study of collagen types and fibronectin in the rat. *Acta Neuropathol.* **67**, 315–321 (1985).
 26. THOMAS, P. K. The connective tissue of peripheral nerve: an electron microscope study. *J. Anat.* **97**, 35–44 (1963).
 27. Sunderland, S. The connective tissues of peripheral nerves. *Brain* **88**, 841–854 (1965).
 28. Jabaley, M. E., Wallace, W. H. & Heckler, F. R. Internal topography of major nerves of the forearm and hand: A current view. *J. Hand Surg. Am.* (1980) doi:10.1016/S0363-5023(80)80035-9.
 29. Nicholls, K. & Furness, N. D. Peripheral nerve compression syndromes of the upper limb. *Surgery (United Kingdom)* vol. 37 288–293 (2019).
 30. Wojtkiewicz, D. M. *et al.* Social impact of peripheral nerve injuries. *Hand* (2015) doi:10.1007/s11552-014-9692-0.
 31. Gordon, T., Tyreman, N. & Raji, M. A. The basis for diminished functional recovery after delayed peripheral nerve repair. *J. Neurosci.* **31**, 5325–5334 (2011).
 32. Burnett, M. G. & Zager, E. L. Pathophysiology of peripheral nerve injury: a brief review. *Neurosurgical focus* vol. 16 (2004).
 33. Seddon, H. J. & Nu, F. R. C. S. *A CLASSIFICATION OF NERVE INJURIES.*
 34. Seddon, H. J. Three types of nerve injury. *Brain* (1943) doi:10.1093/brain/66.4.237.
 35. Kaya, Y. & Sarikcioglu, L. Sir Herbert Seddon (1903-1977) and his classification scheme for peripheral nerve injury. doi:10.1007/s00381-014-2560-y.
 36. Sunderland, S. A classification of peripheral nerve injuries producing loss of function. *Brain* (1951) doi:10.1093/brain/74.4.491.
 37. Mackinnon, S. E. & Dellon, A. L. *Surgery of the Peripheral Nerve.* (Thieme Medical Publishers, 1988).
 38. Farber, S. J. *et al.* Peripheral nerve injury after local anesthetic injection. *Anesth. Analg.* (2013) doi:10.1213/ANE.0b013e3182a00767.
 39. Waller, A. XX. Experiments on the section of the glossopharyngeal and hypoglossal nerves of the frog, and observations of the alterations produced thereby in the structure of their primitive fibres. *Philos. Trans. R. Soc. London* **140**, 423–429 (1850).
 40. Lunn, E. R., Perry, V. H., Brown, M. C., Rosen, H. & Gordon, S. Absence of Wallerian Degeneration does not Hinder Regeneration in Peripheral Nerve. *Eur. J. Neurosci.* **1**, 27–33 (1989).
 41. Araki, T., Sasaki, Y. & Milbrandt, J. Increased nuclear NAD biosynthesis and SIRT1 activation prevent axonal degeneration. *Science (80-.)*. **305**, 1010–1013 (2004).
 42. Fernandes, K. J. L., Fan, D.-P., Tsui, B. J., Cassar, S. L. & Tetzlaff, W. *Influence of the Axotomy to Cell Body Distance in Rat Rubrospinal and Spinal Motoneurons: Differential*

- Regulation of GAP-43, Tubulins, and Neurofilament-M.* *J. Comp. Neurol.* vol. 414 (1999).
43. Koliatsos, V. E., Price, W. L., Pardo, C. A. & Price, D. L. Ventral root avulsion: An experimental model of death of adult motor neurons. *J. Comp. Neurol.* **342**, 35–44 (1994).
 44. Richardson, P. M. *et al.* Responses of the nerve cell body to axotomy. *Neurosurgery* vol. 65 A74–A79 (2009).
 45. VIAL, J. D. The early changes in the axoplasm during wallerian degeneration. *J. Biophys. Biochem. Cytol.* **4**, 551–555 (1958).
 46. Mcquarrie, I. G. & Grafstein, B. Axon Outgrowth Enhanced by a Previous Nerve Injury. *Arch. Neurol.* **29**, 53–55 (1973).
 47. Dahlin, L. B., Necking, L. E., Lundström, R. & Lundborg, G. Vibration exposure and conditioning lesion effect in nerves: An experimental study in rats. *J. Hand Surg. Am.* **17**, 858–861 (1992).
 48. Siskin, B. F., Kanje, M., Lundborg, G., Herbst, E. & Kurtz, W. Stimulation of rat sciatic nerve regeneration with pulsed electromagnetic fields. *Brain Res.* **485**, 309–316 (1989).
 49. Dahlin, L. B. Stimulation of regeneration of the sciatic nerve by experimentally induced inflammation in rats. *Scand. J. Plast. Reconstr. Surg. Hand Surg.* **26**, 121–125 (1992).
 50. Dahlin, L. B. & Kanje, M. Conditioning effect induced by chronic nerve compression. *Scand. J. Plast. Reconstr. Surg. Hand Surg.* **26**, 37–41 (1992).
 51. Qiu, J. *et al.* Spinal axon regeneration induced by elevation of cyclic AMP. *Neuron* **34**, 895–903 (2002).
 52. Hoffman, P. N. & Lasek, R. J. Axonal transport of the cytoskeleton in regenerating motor neurons: constancy and change. *Brain Res.* **202**, 317–333 (1980).
 53. Raivich, G. *et al.* The AP-1 transcription factor c-Jun is required for efficient axonal regeneration. *Neuron* **43**, 57–67 (2004).
 54. Seijffers, R., Allchorne, A. J. & Woolf, C. J. The transcription factor ATF-3 promotes neurite outgrowth. *Mol. Cell. Neurosci.* **32**, 143–154 (2006).
 55. Jankowski, M. P., Miller, L. & Koerber, H. R. Increased Expression of Transcription Factor SRY-box-Containing Gene 11 (Sox11) Enhances Neurite Growth by Regulating Neurotrophic Factor Responsiveness. *Neuroscience* **382**, 93–104 (2018).
 56. Sherman, D. L. & Brophy, P. J. Mechanisms of axon ensheathment and myelin growth. *Nature Reviews Neuroscience* vol. 6 683–690 (2005).
 57. Abercrombie, M. & Johnson, M. L. Quantitative histology of Wallerian degeneration: I. Nuclear population in rabbit sciatic nerve. *J. Anat.* **80**, 37–50 (1946).
 58. Kim, H. A. *et al.* A developmentally regulated switch regenerative growth of Schwann cells through cyclin D1. *Neuron* **26**, 405–416 (2000).
 59. Atanasoski, S., Shumas, S., Dickson, C., Scherer, S. S. & Suter, U. Differential cyclin D1 requirements of proliferating Schwann cells during development and after injury. *Mol. Cell. Neurosci.* **18**, 581–592 (2001).
 60. Parkinson, D. B. *et al.* c-Jun is a negative regulator of myelination. *J. Cell Biol.* **181**, 625–637 (2008).
 61. Stoll, G., Griffin, J. W., Li, C. Y. & Trapp, B. D. Wallerian degeneration in the peripheral nervous system: participation of both Schwann cells and macrophages in myelin degradation. *J. Neurocytol.* **18**, 671–683 (1989).
 62. Ribeiro-Resende, V. T., Koenig, B., Nichterwitz, S., Oberhoffner, S. & Schlosshauer, B. Strategies for inducing the formation of bands of Büngner in peripheral nerve regeneration. *Biomaterials* **30**, 5251–5259 (2009).

63. Heumann, R., Korsching, S., Bandtlow, C. & Thoenen, H. Changes of nerve growth factor synthesis in nonneuronal cells in response to sciatic nerve transection. *J. Cell Biol.* **104**, 1623–1631 (1987).
64. Nieke, J. & Scbachner, M. Expression of the neural cell adhesion molecules L1 and N-CAM and their common carbohydrate epitope L2/HNK-1 during development and after transection of the mouse sciatic nerve. *Differentiation* **30**, 141–151 (1985).
65. Rutkowski, J. L. *et al.* Signals for proinflammatory cytokine secretion by human Schwann cells. *J. Neuroimmunol.* **101**, 47–60 (1999).
66. Rodríguez, F. J., Verdú, E., Ceballos, D. & Navarro, X. Nerve guides seeded with autologous Schwann cells improve nerve regeneration. *Exp. Neurol.* **161**, 571–584 (2000).
67. Henderson, C. E. Role of neurotrophic factors in neuronal development. *Curr. Opin. Neurobiol.* **6**, 64–70 (1996).
68. Cohen, S. & Levi-Montalcini, R. A NERVE GROWTH-STIMULATING FACTOR ISOLATED FROM SNAKE VENOM. *Proc. Natl. Acad. Sci.* **42**, 571–574 (1956).
69. Skaper, S. D. The neurotrophin family of neurotrophic factors: An Overview. *Methods in Molecular Biology* vol. 846 1–12 (2012).
70. Cosgaya, J. M., Chan, J. R. & Shooter, E. M. The neurotrophin receptor p75NTR as a positive modulator of myelination. *Science (80-)*. **298**, 1245–1248 (2002).
71. Boyd, J. G. & Gordon, T. A dose-dependent facilitation and inhibition of peripheral nerve regeneration by brain-derived neurotrophic factor. *Eur. J. Neurosci.* **15**, 613–626 (2002).
72. Heumann, R. *et al.* Differential regulation of mRNA encoding nerve growth factor and its receptor in rat sciatic nerve during development, degeneration, and regeneration: role of macrophages. *Proc. Natl. Acad. Sci. U. S. A.* **84**, 8735–8739 (1987).
73. Funakoshi, H. *et al.* Differential expression of mRNAs for neurotrophins and their receptors after axotomy of the sciatic nerve. *J. Cell Biol.* **123**, 455–465 (1993).
74. Yan, Q., Matheson, C. & Lopez, O. T. In vivo neurotrophic effects of GDNF on neonatal and adult facial motor neurons. *Nature* vol. 373 341–344 (1995).
75. Boyd, J. G. & Gordon, T. Glial cell line-derived neurotrophic factor and brain-derived neurotrophic factor sustain the axonal regeneration of chronically axotomized motoneurons in vivo. *Exp. Neurol.* **183**, 610–619 (2003).
76. Fine, E. G., Decosterd, I., Papaloizos, M., Zurn, A. D. & Aebischer, P. GDNF and NGF released by synthetic guidance channels support sciatic nerve regeneration across a long gap. *Eur. J. Neurosci.* **15**, 589–601 (2002).
77. Seddon, H. J., Medawar, P. B. & Smith, H. Rate of regeneration of peripheral nerves in man. *J. Physiol.* **102**, 191–215 (1943).
78. Bowe, C. M., Hildebrand, C., Kocsis, J. D. & Waxman, S. G. Morphological and physiological properties of neurons after long-term axonal regeneration: observations on chronic and delayed sequelae of peripheral nerve injury. *Journal of the Neurological Sciences* vol. 91 259–292 (1989).
79. Fu, S. Y. & Gordon, T. Contributing Factors to Poor Functional Recovery after Delayed Nerve Repair: Prolonged Axotomy. *J. Neurosci.* **15**, 3876–3885 (1995).
80. Schwab, M. E. & Bartholdi, D. Degeneration and regeneration of axons in the lesioned spinal cord. *Physiological Reviews* vol. 76 319–370 (1996).
81. Silver, J. & Miller, J. H. Regeneration beyond the glial scar. *Nature Reviews Neuroscience* vol. 5 146–156 (2004).
82. Filbin, M. T. Myelin-associated inhibitors of axonal regeneration in the adult mammalian

- CNS. *Nat. Rev. Neurosci.* **4**, 703–713 (2003).
83. Fournier, A. E., GrandPre, T. & Strittmatter, S. M. Identification of a receptor mediating Nogo-66 inhibition of axonal regeneration. *Nature* vol. 409 341–346 (2001).
 84. Wang, K. C. *et al.* Oligodendrocyte-myelin glycoprotein is a Nogo receptor ligand that inhibits neurite outgrowth. *Nature* **417**, 941–944 (2002).
 85. Muir, D. The potentiation of peripheral nerve sheaths in regeneration and repair. *Experimental Neurology* vol. 223 102–111 (2010).
 86. Siebert, J. R., Conta Steencken, A. & Osterhout, D. J. Chondroitin Sulfate Proteoglycans in the Nervous System: Inhibitors to Repair. *BioMed Research International* vol. 2014 (2014).
 87. Braunewell, K. -H *et al.* Functional Involvement of Sciatic Nerve-derived Versican and Decorin-like Molecules and other Chondroitin Sulphate Proteoglycans in ECM-mediated Cell Adhesion and Neurite Outgrowth. *Eur. J. Neurosci.* **7**, 805–814 (1995).
 88. Muir, D., Engvall, E., Varon, S. & Manthorpe, M. Schwannoma cell-derived inhibitor of the neurite-promoting activity of laminin. *J. Cell Biol.* **109**, 2353–2362 (1989).
 89. Sharma, K., Selzer, M. E. & Li, S. Scar-mediated inhibition and CSPG receptors in the CNS. *Experimental Neurology* vol. 237 370–378 (2012).
 90. Bertolotto, A., Palmucci, L., Gagliano, A., Mongini, T. & Tarone, G. Immunohistochemical localization of chondroitin sulfate in normal and pathological human muscle. *J. Neurol. Sci.* **73**, 233–244 (1986).
 91. Zuo, J. *et al.* Regeneration of axons after nerve transection repair is enhanced by degradation of chondroitin sulfate proteoglycan. *Exp. Neurol.* **176**, 221–228 (2002).
 92. Zuo, J., Ferguson, T. A., Hernandez, Y. J., Stetler-Stevenson, W. G. & Muir, D. Neuronal matrix metalloproteinase-2 degrades and inactivates a neurite-inhibiting chondroitin sulfate proteoglycan. *J. Neurosci.* **18**, 5203–5211 (1998).
 93. Brown, J. M. & Mackinnon, S. E. Nerve Transfers in the Forearm and Hand. *Hand Clinics* (2008) doi:10.1016/j.hcl.2008.08.002.
 94. Paskal, A. M. *et al.* Novel model of somatosensory nerve transfer in the rat. in *Advances in Experimental Medicine and Biology* (2018). doi:10.1007/5584_2018_209.
 95. Gordon, T. *et al.* Nerve Cross-Bridging to Enhance Nerve Regeneration in a Rat Model of Delayed Nerve Repair. *PLoS One* **10**, e0127397 (2015).
 96. Viterbo, F., Trindade, J. C., Hoshino, K. & Mazzoni Neto, A. Latero-terminal neurotomy without removal of the epineurial sheath. Experimental study in rats. *Rev. Paul. Med.* (1992).
 97. Hayashi, A. *et al.* Axotomy or compression is required for axonal sprouting following end-to-side neurotomy. *Exp. Neurol.* (2008) doi:10.1016/j.expneurol.2008.02.031.
 98. Hill, E. J. R. & Fox, I. K. Current best peripheral nerve transfers for spinal cord injury. *Plast. Reconstr. Surg.* **143**, 184E–198E (2019).
 99. Dunn, J. C. *et al.* Supercharge End-to-Side Nerve Transfer: Systematic Review. *HAND* (2019) doi:10.1177/1558944719836213.
 100. Davidge, K. M., Yee, A., Moore, A. M. & Mackinnon, S. E. The supercharge end-to-side anterior interosseous-to-ulnar motor nerve transfer for restoring intrinsic function: Clinical experience. in *Plastic and Reconstructive Surgery* (2015). doi:10.1097/PRS.0000000000001514.
 101. Power, H. A. *et al.* Refining Indications for the Supercharge End-to-Side Anterior Interosseous to Ulnar Motor Nerve Transfer in Cubital Tunnel Syndrome. *Plast. Reconstr.*

- Surg.* (2020) doi:10.1097/PRS.0000000000006399.
102. Roskoski, R. The ErbB/HER family of protein-tyrosine kinases and cancer. *Pharmacological Research* vol. 79 34–74 (2014).
 103. Citri, A., Skaria, K. B. & Yarden, Y. The deaf and the dumb: The biology of ErbB-2 and ErbB-3. *Experimental Cell Research* vol. 284 54–65 (2003).
 104. Ferguson, K. M. *et al.* EGF activates its receptor by removing interactions that autoinhibit ectodomain dimerization. *Mol. Cell* **11**, 507–517 (2003).
 105. Cho, H. S. & Leahy, D. J. Structure of the extracellular region of HER3 reveals an interdomain tether. *Science (80-.)*. **297**, 1330–1333 (2002).
 106. Yarden, Y. & Sliwkowski, M. X. Untangling the ErbB signalling network. *Nature Reviews Molecular Cell Biology* vol. 2 127–137 (2001).
 107. Downward, J. *et al.* Close similarity of epidermal growth factor receptor and v-erb-B oncogene protein sequences. *Nature* **307**, 521–527 (1984).
 108. Yang, L., Li, Y. & Zhang, Y. Identification of prolidase as a high affinity ligand of the ErbB2 receptor and its regulation of ErbB2 signaling and cell growth. *Cit. Cell Death Dis.* **5**, (2014).
 109. Singh, B., Carpenter, G. & Coffey, R. J. EGF receptor ligands: Recent advances [version 1; referees: 3 approved]. *F1000Research* vol. 5 (2016).
 110. Pinkas-Kramarski, R. *et al.* Diversification of Neu differentiation factor and epidermal growth factor signaling by combinatorial receptor interactions. *EMBO J.* **15**, 2452–2467 (1996).
 111. Burden, S. & Yarden, Y. Neuregulins and their receptors: A versatile signaling module in organogenesis and oncogenesis. in *Neuron* vol. 18 847–855 (Cell Press, 1997).
 112. Tzahar, E. *et al.* A hierarchical network of interreceptor interactions determines signal transduction by Neu differentiation factor/neuregulin and epidermal growth factor. *Mol. Cell. Biol.* **16**, 5276–5287 (1996).
 113. Garrett, T. P. J. *et al.* The crystal structure of a truncated ErbB2 ectodomain reveals an active conformation, poised to interact with other ErbB receptors. *Mol. Cell* **11**, 495–505 (2003).
 114. PENUEL, E. Structural requirements for ErbB2 transactivation. *Semin. Oncol.* **28**, 36–42 (2001).
 115. Ross, J. S. *et al.* The HER-2 Receptor and Breast Cancer: Ten Years of Targeted Anti-HER-2 Therapy and Personalized Medicine LEARNING OBJECTIVES. (2009) doi:10.1634/theoncologist.2008-0230.
 116. Guy, P. M., Platko, J. V., Cantley, L. C., Cerione, R. A. & Carraway, K. L. Insect cell-expressed p180(erbB3) possesses an impaired tyrosine kinase activity. *Proc. Natl. Acad. Sci. U. S. A.* **91**, 8132–8136 (1994).
 117. Fricker, F. R. & Bennett, D. L. The role of neuregulin-1 in the response to nerve injury. *Future Neurology* vol. 6 809–822 (2011).
 118. Bouyain, S., Longo, P. A., Li, S., Ferguson, K. M. & Leahy, D. J. The extracellular region of ErbB4 adopts a tethered conformation in the absence of ligand. *Proc. Natl. Acad. Sci. U. S. A.* **102**, 15024–15029 (2005).
 119. Plowman, G. D. *et al.* Ligand-specific activation of HER4/p180erbB4, a fourth member of the epidermal growth factor receptor family. *Proc. Natl. Acad. Sci. U. S. A.* **90**, 1746–1750 (1993).
 120. Gassmann, M. *et al.* Aberrant neural and cardiac development in mice lacking the ErbB4

- neuregulin receptor. *Nature* **378**, 390–394 (1995).
121. Fendly, B. M. *et al.* Characterization of Murine Monoclonal Antibodies Reactive to Either the Human Epidermal Growth Factor Receptor or HER2/neu Gene Product. *Cancer Res.* **50**, (1990).
 122. Cho, H. S. *et al.* Structure of the extracellular region of HER2 alone and in complex with the Herceptin Fab. *Nature* **421**, 756–760 (2003).
 123. Hudziak, R. M. *et al.* p185HER2 monoclonal antibody has antiproliferative effects in vitro and sensitizes human breast tumor cells to tumor necrosis factor. *Mol. Cell. Biol.* **9**, 1165–1172 (1989).
 124. BASELGA, J. Mechanism of action of trastuzumab and scientific update. *Semin. Oncol.* **28**, 4–11 (2001).
 125. Slamon, D. J. *et al.* Use of Chemotherapy plus a Monoclonal Antibody against HER2 for Metastatic Breast Cancer That Overexpresses HER2. *N. Engl. J. Med.* **344**, 783–792 (2001).
 126. Andersson, M. *et al.* Phase III randomized study comparing docetaxel plus trastuzumab with vinorelbine plus trastuzumab as first-line therapy of metastatic or locally advanced human epidermal growth factor receptor 2-positive breast cancer: The HERNATA study. *J. Clin. Oncol.* **29**, 264–271 (2011).
 127. Keefe, D. L. Trastuzumab-associated cardiotoxicity. *Cancer* **95**, 1592–1600 (2002).
 128. Higa, G. M. & Abraham, J. Lapatinib in the treatment of breast cancer. *Expert Review of Anticancer Therapy* vol. 7 1183–1192 (2007).
 129. Geyer, C. E., Forster, J. & Lindquist, D. Lapatinib plus capecitabine for HER2-positive advanced breast cancer. *Advances in Breast Cancer* vol. 5 45 (2008).
 130. Segovia-Mendoza, M., González-González, M. E., Barrera, D., Díaz, L. & García-Becerra, R. Efficacy and mechanism of action of the tyrosine kinase inhibitors gefitinib, lapatinib and neratinib in the treatment of her2-positive breast cancer: Preclinical and clinical evidence. *American Journal of Cancer Research* vol. 5 2531–2561 (2015).
 131. Wakeling, A. E. *et al.* ZD1839 (Iressa): An orally active inhibitor of epidermal growth factor signaling with potential for cancer therapy. *Cancer Res.* **62**, 5749–5754 (2002).
 132. Lynch, T. J. *et al.* Activating Mutations in the Epidermal Growth Factor Receptor Underlying Responsiveness of Non-Small-Cell Lung Cancer to Gefitinib. *N. Engl. J. Med.* **350**, 2129–2139 (2004).
 133. Pearson, R. J. & Carroll, S. L. ErbB Transmembrane Tyrosine Kinase Receptors Are Expressed by Sensory and Motor Neurons Projecting into Sciatic Nerve. *J. Histochem. Cytochem.* **52**, 1299–1311 (2004).
 134. Nave, K. A. & Salzer, J. L. Axonal regulation of myelination by neuregulin 1. *Current Opinion in Neurobiology* vol. 16 492–500 (2006).
 135. Chang, H. M. *et al.* Neuregulin Facilitates Nerve Regeneration by Speeding Schwann Cell Migration via ErbB2/3-Dependent FAK Pathway. *PLoS One* **8**, e53444 (2013).
 136. Riethmacher, D. *et al.* Severe neuropathies in mice with targeted mutations in the ErbB3 receptor. *Nature* **389**, 725–730 (1997).
 137. Garratt, A. N., Voiculescu, O., Topilko, P., Charnay, P. & Birchmeier, C. A dual role of erbB2 in myelination and in expansion of the Schwann cell precursor pool. *J. Cell Biol.* **148**, 1035–1046 (2000).
 138. Fricker, F. R. *et al.* Axonally derived neuregulin-1 is required for remyelination and regeneration after nerve injury in adulthood. *J. Neurosci.* **31**, 3225–3233 (2011).

139. Michailov, G. V. *et al.* Axonal Neuregulin-1 Regulates Myelin Sheath Thickness. *Science* (80-.). **304**, 700–703 (2004).
140. Atanasoski, S. *et al.* ErbB2 signaling in Schwann cells is mostly dispensable for maintenance of myelinated peripheral nerves and proliferation of adult Schwann cells after injury. *J. Neurosci.* **26**, 2124–2131 (2006).
141. Audisio, C. *et al.* ErbB receptors modulation in different types of peripheral nerve regeneration. *Neuroreport* **19**, 1605–1609 (2008).
142. Ahmed, Z., Jacques, S. J., Berry, M. & Logan, A. Epidermal growth factor receptor inhibitors promote CNS axon growth through off-target effects on glia. *Neurobiol. Dis.* **36**, 142–150 (2009).
143. Douglas, M. R. *et al.* Off-target effects of epidermal growth factor receptor antagonists mediate retinal ganglion cell disinhibited axon growth. *Brain* **132**, 3102–3121 (2009).
144. Leinster, V. H. L., Joy, M. T., Vuononvirta, R. E., Bolsover, S. R. & Anderson, P. N. ErbB1 epidermal growth factor receptor is a valid target for reducing the effects of multiple inhibitors of axonal regeneration. *Exp. Neurol.* **239**, 82–90 (2013).
145. Placheta, E. *et al.* The ErbB2 inhibitor Herceptin (Trastuzumab) promotes axonal outgrowth four weeks after acute nerve transection and repair. *Neurosci. Lett.* (2014) doi:10.1016/j.neulet.2014.09.006.
146. Karsy, M. *et al.* Trends and Cost Analysis of Upper Extremity Nerve Injury Using the National (Nationwide) Inpatient Sample. *World Neurosurg.* (2019) doi:10.1016/j.wneu.2018.11.192.
147. Hudachek, S. F. & Gustafson, D. L. Physiologically based pharmacokinetic model of lapatinib developed in mice and scaled to humans. *J. Pharmacokinet. Pharmacodyn.* **40**, 157–176 (2013).
148. KS, T. *et al.* Lapatinib distribution in HER2 overexpressing experimental brain metastases of breast cancer. *Pharm. Res.* **29**, 770–781 (2012).
149. Stewart, C. F. *et al.* Gefitinib Enhances the Antitumor Activity and Oral Bioavailability of Irinotecan in Mice. *Cancer Res.* **64**, 7491–7499 (2004).
150. Q, Z. *et al.* Effect of weekly or daily dosing regimen of Gefitinib in mouse models of lung cancer. *Oncotarget* **8**, 72447–72456 (2017).
151. Abercrombie, M. Estimation of nuclear population from microtome sections. *Anat. Rec.* **94**, 239–247 (1946).
152. More, H. L., Chen, J., Gibson, E., Donelan, J. M. & Beg, M. F. A semi-automated method for identifying and measuring myelinated nerve fibers in scanning electron microscope images. *J. Neurosci. Methods* **201**, 149–158 (2011).
153. Sleight, J. N., Weir, G. A. & Schiavo, G. A simple, step-by-step dissection protocol for the rapid isolation of mouse dorsal root ganglia. *BMC Res. Notes* **9**, (2016).
154. Meijering, E. *et al.* Design and Validation of a Tool for Neurite Tracing and Analysis in Fluorescence Microscopy Images. *Cytom. Part A* **58**, 167–176 (2004).
155. SW, K., PS, C. & R, M. Comparative outcome measures in peripheral regeneration studies. *Exp. Neurol.* **287**, 348–357 (2017).
156. Schmalbruch, H. Fiber composition of the rat sciatic nerve. *Anat. Rec.* **215**, 71–81 (1986).
157. Ronchi, G. *et al.* The median nerve injury model in pre-clinical research – A critical review on benefits and limitations. *Frontiers in Cellular Neuroscience* vol. 13 (2019).
158. Navarro, X. Functional evaluation of peripheral nerve regeneration and target reinnervation in animal models: A critical overview. *European Journal of Neuroscience*

- vol. 43 271–286 (2016).
159. Weber, R. A., Proctor, W. H., Warner, M. R. & Verheyden, C. N. Autotomy and the sciatic functional index. *Microsurgery* **14**, 323–327 (1993).
 160. Bertelli, J. A., Taleb, M., Saadi, A., Mira, J. -C & Pecot-Dechavassine, M. The rat brachial plexus and its terminal branches: An experimental model for the study of peripheral nerve regeneration. *Microsurgery* **16**, 77–85 (1995).
 161. Bertelli, J. A. & Mira, J. C. The grasping test: a simple behavioral method for objective quantitative assessment of peripheral nerve regeneration in the rat. *J. Neurosci. Methods* **58**, 151–155 (1995).
 162. Papalia, I., Tos, P., D’Alcontres, F. S., Battiston, B. & Geuna, S. On the use of the grasping test in the rat median nerve model: A re-appraisal of its efficacy for quantitative assessment of motor function recovery. *J. Neurosci. Methods* **127**, 43–47 (2003).
 163. Green, E. *Anatomy of the Rat*. (Hafner, 1959).
 164. Moore, A. M. *et al.* A transgenic rat expressing green fluorescent protein (GFP) in peripheral nerves provides a new hindlimb model for the study of nerve injury and regeneration. *J. Neurosci. Methods* **204**, 19–27 (2012).
 165. Kemp, S. W. P. *et al.* Functional recovery following peripheral nerve injury in the transgenic Thy1 -GFP rat. in *Journal of the Peripheral Nervous System* vol. 18 220–231 (J Peripher Nerv Syst, 2013).
 166. Jager, S. B., Ronchi, G., Vaegter, C. B. & Geuna, S. The mouse median nerve experimental model in regenerative research. *Biomed Res. Int.* **2014**, (2014).
 167. Kaplan, S., Geuna, S., Ronchi, G., Ulkay, M. B. & von Bartheld, C. S. Calibration of the stereological estimation of the number of myelinated axons in the rat sciatic nerve: A multicenter study. *J. Neurosci. Methods* **187**, 90–99 (2010).
 168. Deniz, Ö. G. *et al.* A concise review of optical, physical and isotropic fractionator techniques in neuroscience studies, including recent developments. *Journal of Neuroscience Methods* vol. 310 45–53 (2018).
 169. Hendry, J. M., Cecilia Alvarez-Veronesi, M., Chiang, C., Gordon, T. & Borschel, G. H. Neurofilament-histomorphometry comparison in the evaluation of unmyelinated axon regeneration following peripheral nerve injury: An alternative to electron microscopy. *J. Neurosci. Methods* **320**, 37–43 (2019).
 170. Rushton, W. A. H. A theory of the effects of fibre size in medullated nerve. *J. Physiol.* **115**, 101–122 (1951).